AD 690912

NOLTR 69-235

COMPARISON OF CURVATURE OF DETONATION FRONT IN AP WITH THAT FOUND IN SOME CONVENTIONAL EXPLOSIVES

By
J. O. Erkman
Donna Price

DDC
RECEIVED
AUG 18 1970
A

25 MAY 1970

NOL

UNITED STATES NAVAL ORDNANCE LABORATORY, WHITE OAK, MARYLAND

NOLTR 69-235

ATTENTION

This document has been approved for public release and sale, its distribution is unlimited.

57

NOLTR 69-235

COMPARISON OF CURVATURE OF DETONATION FRONT IN AP WITH THAT FOUND IN SOME CONVENTIONAL EXPLOSIVES

J. O. Erkman and Donna Price

ABSTRACT: The original purpose of this work was to obtain data necessary for the design of experiments in which particle velocity (u) could be measured by a new electromagnetic method. It was soon apparent that a knowledge of the curvature of the detonation front was needed for the measurement of detonation velocity as well as for u. Hence, we have studied 50-51 mm diameter charges of AP, NQ, TNT, and RDX to provide the necessary data. The most important result of the work is the finding that the detonation front acquires a constant curvature after a fairly short run in AP charges and also in some low density conventional explosives.

Working Group: D. J. Edwards, J. O. Erkman, D. Price, and A. R. Clairmont, Jr.

PUBLISHED 25 MAY 1970

Approved by:

CARL BOYARS, CHIEF
Advanced Chemistry Division
CHEMISTRY RESEARCH DEPARTMENT
U. S. NAVAL ORDNANCE LABORATORY
White Oak, Silver Spring, Maryland

NOLTR 69-235 25 May 1970

COMPARISON OF CURVATURE OF DETONATION FRONT IN AP WITH THAT FOUND IN SOME CONVENTIONAL EXPLOSIVES

This work was initiated under MAT-03L-000/ZR011-01-01 and was concluded under that project and ORD-331-002/UF19-332-302. The report is concerned with the curvature of the detonation fronts in 50 mm diameter charges of AP, NQ, TNT, RDX and Tetryl. These data will be of interest to those who measure the velocity of detonating charges by observing the detonations with a camera. The data also have interesting implications for consideration in theoretical treatments of detonations in cylindrical charges.

GEORGE G. BALL
Captain, USN
Commander

Albert F. Lightbody

ALBERT LIGHTBODY
By direction

TABLE OF CONTENTS

TABLE OF CONTENTS (cont'd)

ILLUSTRATIONS

TABLE OF CONTENTS (cont'd)

TABLES

NOLTR 69-235

COMPARISON OF CURVATURE OF DETONATION FRONT IN AP WITH THAT FOUND IN SOME CONVENTIONAL EXPLOSIVES

INTRODUCTION

Previous work has shown that the radius of curvature (R_c) of the detonation front in point-initiated tetryl (ρ_o = 1.51 g/cc) cylinders increases with cylinder length (ℓ) in the manner to be expected for spherical expansion of the front.[1] Up to the largest charge fired (ℓ/d of 4 for d = 50.8 mm), where d is the charge diameter, this direct proportionality between R_c and ℓ was observed. On the other hand, Cook reported[2] for fine-grained, low density, "ideal" explosives that the region of spherical expansion is followed by a decaying rate of expansion until a constant curvature is reached and maintained at and above (ℓ/d) ~ 3.5. For "non-ideal" explosives (e.g., very coarse, low density TNT and coarse TNT/sodium nitrate, 50/50), the change from spherical expansion to constant curvature is abrupt and occurs at ℓ/d of 1.5 - 2.0.

Earlier, we developed a correction to our measured detonation velocities to compensate for the curvature of the initiating shock front.[3] This correction was derived on the assumption of uninterrupted spherical expansion of the detonation front. Consequently the validity of this correction depends upon its application only to explosives exhibiting such behavior. Thus, one objective of the present study was to examine R_c vs ℓ/d data of several explosives to determine which ones exhibit the spherically expanding fronts.

Another objective was to obtain the detailed information about curvature of the detonation front needed to interpret correctly (as particle velocity) the measurements obtained by the electromagnetic method. This method is in process of development; it depends on a thin metal foil moving at the material velocity of the front. Best results (no correction) will be obtained for planar detonation fronts. Acceptable results can be obtained by correcting the measurements according to independently measured R_c. The curvature must be known, must be reproducible,

and must be small enough to set a practical length of foil (e.g., 5 - 10 mm) into uniform motion within a very small delay period (e.g., 30 nsec.). In particular we wished to know R_c of ammonium perchlorate (AP) as a function of particle size (δ), loading density (ρ_0), and charge length so that the electromagnetic method can be used to study what is generally considered to be the relatively long reaction zone of this explosive.

In addition to the primary objectives of obtaining R_c data necessary for the electromagnetic method and for valid corrections of our detonation measurements we wished to examine any appropriate curvature data in the theories[4,5] which relate R_c to reaction zone length, a. Few applications of these theories have been made because appropriate R_c data are not usually available.

EXPERIMENTAL

Materials

Five batches of AP were used in this work; all were of the propellant grade and contained 0.2 - 0.5% tricalcium phosphate (TCP). Four batches, freshly ground on the same schedule at the Naval Ordnance Station, Indian Head, Maryland, had a nominal average particle size of 9 μ by micromerograph. These were N136 (8.4 μ), N138 (8.9 μ), N139 (8.8 μ) and N140 (8.3 μ). The fifth batch, N126 was originally assigned an average particle size of 25 μ[6] when it was acquired several years ago. After putting a sample of this material through a coarse screen to remove a few large agglomerates, NOS reports that its micromerograph value is still 25 μ.

Three organic H.E. were used in this work and all were procured under the respective military specifications. RDX, X659, was ordered as Type B Class E (98% through a No. 325 screen) Holston Production; an analogous lot of HMX had a weight mean particle size of 14 μ. TNT, X517, is a coarse H.E. with a mean δ of 200 μ; see Table 7. Nitroguanidine (NQ) X547 is the low bulk density form described and used in earlier work.[7]

Pressed Charge Preparation

The explosives were handled and made into cylindrical charges as in the previous work[8] except that AP charges were given special treatment to avoid moisture pick-up. In preparing these charges, AP was taken directly from moisture-vapor proof storage bags and loaded directly into the mold; if for any reason AP required drying, it was dried in a vacuum oven. Any AP charges not fired as soon as possible after preparation were packaged in Saran and stored at 30°C until they could be fired.

In the present work, the charge diameter was kept at 50 - 51 mm, but both length and the loading density were varied. The total charge train was made up of a detonator (Engineers Special Hercules J-2), a 50/50, 1.56 g/cc pentolite booster (diam. of main charge, 25.4 mm long), and the main charge. In detonation velocity measurements, the main charge was generally followed by a second booster pellet to serve as an explosive witness.

Measurements

A 70 mm smear camera (writing speed about 4 mm/μsec) was used to measure both the detonation velocity (D) and the radius of curvature. All records were made with Tri-X film developed in Acufine.

For measurements of D, the charge was mounted vertically with the detonator at the top. In a very few cases, Magic Tape was used as a flasher*. The usual procedure and typical records are described in previous work.[8]

For measurements of R_c, the charge was mounted horizontally on a Styrofoam V-block. The camera slit was focused on the end face of the main charge, and was perpendicular to the charge axis. The maximum writing speed of 4 mm/μ sec was

* If possible, a flasher is avoided. For granular charges, especially those with chalky surfaces, it is difficult to produce an air gap of uniform thickness and hence a record of uniform luminosity.

used but, even so, the horizontal (time) component of the trace varied only from 2 to 11 mm on the film. Obviously a higher writing speed would improve this measurement. Good traces were obtained without using a flasher. Fig. 1 shows two typical records.

Data Reduction

Reading and reduction of the smear camera velocity records is briefly described in Ref. 8. Details of using the Universal Telereader and auxiliary equipment are set out in Ref. 9. Thirty to 40 points were read on each record for the work reported here. For the most part, the distance-time data were fitted to a straight line (by a least squares procedure) in order to determine the detonation velocity. The use of the straight line was justified by the adequacy of the fit. For short charges, a quadratic was fitted to the data, also by least squares. The velocity at any given point on the observed part of the charge was then determined by evaluating the derivative of the quadratic.

The wave front records were read on the same machine as the velocity records. The cross wires are set on the streak camera trace as shown in Fig. 1b. That is, the vertical wire is set on the left-most part of the trace, so it coincides with line $\overline{ab}$. Then the horizontal wire is moved up to a point where the trace is distinct, point p. Thus point p is the origin for the readings, and about 40 points are read across the trace. Any tilt of the slit with respect to the axis of rotation of the camera mirror is compensated for by reading the coordinates of the ends of the image of the slit, $\overline{ef}$ and $\overline{gh}$.

The ordinates of the upper and lower edges of the image of the end of the charge are also recorded. The horizontal wire is set successively on $\overline{ij}$ and $\overline{kl}$. These latter are used to locate the center of the charge so that the origin for the trace can be moved to point o, see Fig. 1b, and the line $\overline{ot}$ is the time axis. The scale in the picture is read to give the proportionality between distance on

the charge to distance on the screen of the Telereader. The writing speed of the camera and the magnification of the film in the Telereader give the factor required to compute time from the values of the abscissa as read.

In previous work at NOL[1], data similar to those described above were found to represent a spherically expanding front; in cross section, the fronts were circular. Also, Cook[2] found that short charges of numerous explosives gave spherically expanding fronts. For longer charges, however, Cook found that although the fronts were spherical, the radius of curvature did not increase with charge length. Thus it was expected that the data from the present work could be represented by a circle (because we observe a cross section). This was confirmed by the adequacy of the corresponding fit obtained. See Fig. 2 for the results for the two shots represented by the photographs in Fig. 1a and 1b.

When the front shows continuous spherical expansion, the curvature is unsteady in the sense that it changes with additional charge length. The change with length will, however, decrease with increasing charge length. In contrast to this behavior, some charges show a spherical expansion of the front only for short distances, after which R_c becomes constant and independent of length of travel. It is important to be able to recognize these two different modes of propagation. This can be done by superimposing streak camera records which have been taken on charges of different length (after minor corrections for tilt and differences in magnification have been made). If the records coincide, the front is steady for that material and geometry.

Another way of determining if the shape of the detonation front is constant is to observe the velocity of detonation with the streak camera. It has been shown[10] that for a spherically expanding front, this method gives an apparent velocity which is greater than the actual detonation velocity. An alternate statement is that when the velocity along the periphery of a cylinder is not

constant, the front may be expanding spherically. Thus careful measurements of the velocity along the periphery of a charge can, in principle, be used to distinguish between steady and unsteady curvature of the detonation front. We may not have sufficient resolution to see any change in D with spherical expansion; in most cases, D appeared to be constant within our limits of resolution.

The radius of curvature is computed in different ways for the two cases discussed above. The radial expansion case is diagrammed in Fig. 3a where the detonation front has just reached the end of the charge. The radius of curvature is R_c, the distances $\overline{ab}$ and $\overline{ac}$. It is assumed that the detonation velocity, D, is known, and constant, so that $\overline{cd}$ is D x t, where t is the time measured from the appearance of the front at point b. This time at off-axis point d, t_d, and the abscissa, x_d are known from the streak camera record. Thus

$$R_c^2 + x_d^2 = (R_c + D \times t_d)^2 \qquad (1)$$

so that R_c could possibly be computed from only one point on the record. More representative results are obtained by using the method of least squares so that the subscript d takes on all integer values from 1 to the total number of points read on the film.

Note that in Fig. 3a, the front propagates in the direction of its normal. For the steady case, see Fig. 3b, the front moves as a rigid body so that $\overline{cd}$ is D x t and the path is parallel to the axis of the charge. For this case the coordinates of a point on the front, such as c, are given by $(x_d, - D \times t_d)$, where both x_d and t_d represent a particular point on the trace. All data points are treated in this way so that a new set of data is generated which represents the arc shown in Fig. 3b. These are used to evaluate h, k, and R_c in the equation of a circle,

$$(x - h)^2 + (y - k)^2 = R_c^2 \qquad (2)$$

by least squares. This generalized equation permits us to obtain better fits to data from charges which, for one reason or another, are not perfectly uniform or perfectly aligned in the optical system. It also helps to compensate for small asymmetries which can be introduced by the detonators, i.e., these only approximate point initiation. Fig. 2 shows the results obtained from the records shown in Fig. 1 for AP charges which exhibit a constant R_c. In this figure, the solid line trace is for data smoothed to fit Eq. (2). The points shown are derived (see above) from the actual readings of the records.

The adequacy of the fit for either Eq. (1) or (2) is determined by examining plots such as Figs. 2a and 2b, and the computed q.m.e. (quadratic mean error), which is

$$\text{q.m.e.} = \left[\sum_{i=1}^{n} (y_i - y_{ic})^2\right]^{\frac{1}{2}} / (n - p) \qquad (3)$$

where y_i = observed value of ordinate

y_{ic} = value of ordinate computed from the fitted equation

n = number of data points

p = number of parameters in the equation to be fitted

Values of the q.m.e. have all been in an acceptable range; for example, the values for the fits shown in Fig. 2 are 0.13 mm for values of y which vary from -25 to +25 mm. The computer also gives an estimate of the standard deviation of each of the parameters being estimated[11]. These have been converted to percentages and are reported in the tables listing the results.

RESULTS AND DISCUSSION

Detonation Velocity as a Function of Density

D vs ρ_o curves were obtained on the 9 and 25μ AP at d ~ 50 mm, the constant diameter selected for studying the curvature of the front. Data for the 9μ material were obtained on batches N136 and N138, both ground on the same schedule at NOS; these two batches are assumed almost indistinguishable in behavior. Data

for the 25μ AP were obtained on N126 for which a curve had been obtained several years ago.[6] In view of some evidence that the behavior of AP changes with age[12], it was felt that a second determination was necessary. The data obtained are given in Table 1 and plotted in Fig. 4. These D values have not been corrected for non-planar initiation because, as the next section will show, such a correction is not valid for these AP charges.

In similar studies of other H.E., in particular NQ[7], the method of charge preparation has seemed to affect some of the results. Consequently, the method of compaction (by hand, by hydraulic press, or by isostatic press) has been indicated on the graphs as well as in the tables. The trends (D vs ρ_o) of Fig. 4 seem continuous despite changes from one method of charge preparation to another. The curve for the fine AP parallels the ideal curve in the range 0.6 to 1.2 g/cc after which it shows a moderate bending until it ends. The charge at 1.41 g/cc failed, but this does not necessarily mean that the critical density has been exceeded. In this work we are using only half the booster length used in earlier work.[8] Hence the failure could result from inadequate boostering or from exceeding the critical density. The former seems more probable because the present 9μ AP D vs ρ_o curve (d ~ 50 mm) almost coincides with the 10μ AP curve at d = 76 mm, $\rho_o \leq 1.3$ g/cc in the previous work. This is an indication that the 9μ AP is finer than the 10μ AP as, of course, it should be. For the same reason its detonability curve should lie at lower values of d_c and higher values of ρ_c than the curve of the less fine material. Finally, the 10μ AP at d = 50.8 mm, had $\rho_c \simeq 1.475$ g/cc; consequently, the 9μ AP should have $\rho_c \gg 1.48$ g/cc at d ~ 50 mm.

It is not important for the present work to determine ρ_c for this 9μ AP at d ~ 50 mm, and no effort has been made to do so. However, it is of interest that

in the gap test confinement, this AP detonates at 1.584 g/cc[12] and fails (is dead pressed) at 1.590 g/cc. The critical density in the confinement of the gap test must, therefore, be quite near 1.59 g/cc. These limits were determined with pin measurements which resulted in two good examples of the failing reaction obtained in strongly boostered AP when experimental conditions make it sub-critical. Table 2 and Fig. 5 show the fading reactions observed in AP (N138).

The curve for the 25μ AP is very similar to that obtained when this material was first studied. In fact, it is identical at and to the right (toward higher ρ_o) of the maximum in D. The difference appears at lower densities and amounts, at most, to 0.14 mm/μsec. Several years of aging has reduced D at the lowest ρ_o (0.9 g/cc) by this amount. These data and one other example of an aging effect in a finer AP, given in the Appendix, confirm the aging effect suggested in Appendix B of Ref. (12). The particle size effect on D is the same order of magnitude as that established in previous work.[6]

Radius of Curvature as a Function of Density

Table 3 contains the data R_c vs ρ_o obtained for the 9μ and 25μ AP. The radius of curvature was computed in two ways: (1) fitting all the x-y data across the charge surface (d ~ 50 mm) to Eq. 2, and (2) fitting only half the data covering the inner portion of the charge surface (d ~ 25 mm) to Eq. 2. This was done because the quite commonly used curved front theory of Eyring et al[5], proposes a large edge effect. In fact, the effect in the theory as originally formulated is so large that its presence would make a fit of all data to either equation meaningless.

Examination of the data of Table 3 shows that it is quite possible to fit most of the x-y data over the entire surface with a percent error of 1.6% R_c or less. The analogous fit for the central part of the same surface does give a somewhat greater R_c which may indicate a small edge effect. (Many records,

typified by Fig. 2, show a small but definite increase in the curvature of the front as it approaches the charge surface). The percent error, in this case, is somewhat larger than that for treating the whole surface, but generally only to the extent that would be expected by halving the number of measurements treated. If the large edge effect exists, it cannot be resolved on our records. R_c determined by either method showed the same trends. Hence we chose to work here with that determined across the entire charge surface with the advantage of its smaller percent error. Only values so determined are tabulated and plotted in the rest of the report.

The change in curvature noted above is not consistent with the Wood & Kirkwood[4] theory nor with the Eyring[5] theory. However, these data may be useful in modifying the theories as time permits. For example, a condition can be put on the way the detonation front meets the edge of the charge in the Eyring theory. This results in a major reduction of the computed curvature. It is not known if the theory of Wood and Kirkwood can be modified to give radii of curvature whose values differ at the edge of the charge from that at the center of the charge. For these reasons, the radii of curvature over the central half of the AP charge faces, given in Table 3, may be useful in testing any future modification of the curvature theories.

Fig. 6 shows the plot of R_c vs ρ_o for the 9 μ and 25 μ AP. The small variations in diameter (2% or less) have been ignored on the assumption that any corresponding effect on R_c would be undetectable. No distinction has been made in charge lengths of 203 to 457 mm because, as data in the next section will show, charges from both batches of AP attain and maintain a constant R_c over this range of length. As in the case of Fig. 4 (D vs ρ_o), the method of charge preparation has been indicated in Fig. 6 It seems to have more effect on R_c than on D.

Over the range of loading density for which charges were compacted in the isostatic press, the trend shown in Fig. 6 for both batches of AP is a decrease

in R_c (increase in curvature) with an increase in ρ_o. This is opposite in direction to the trend Cook[2] reported for "ideal" explosives; he gives R_c values for the "non-ideal" at only one density. Fig. 6 shows a particle size effect on R_c; for charges compacted in the isostatic press, R_c decreases with increase in initial particle size. This is the trend reported by Cook for both ideal and non-ideal explosives.

For the finer AP (N138), the trend found with the charges prepared in the isostatic press can be reasonably extrapolated to the ρ_o range of the charges prepared in the hydraulic press (See dashed line of Fig. 6). The scatter of the data in the latter region seems a bit more than twice that of the former. This agrees with the poorer reproducibility found in hydraulically pressed charges. For the coarser AP (N126), no analogously reasonable extrapolation is available on going from charges prepared in the isostatic press to those which were hand-packed. For this material, loose packing seems to overwhelm the density effect shown by pressed charges.

Within the higher density region (1.19 to 1.38 g/cc) where the data seem to establish valid trends, there is no apparent correlation between R_c and D. In particular, R_c does not, like D, show a change indicating an approach to failure conditions nor does it extrapolate to a value as low as 0.5 d (25 mm) at ρ_c the R_c reported at d_c.[2]

Variation of R_c with Charge Length

Perhaps the most interesting result of the present study is the variation of R_c with charge length found for several explosives. These will be described in turn.

AP

Table 4 contains radii of curvature for both 9 μ and 25 μ AP in charges varying in length, ℓ, from 2.5 to 23.0 cm. Values of R_c in the fifth column are determined from fitting Eq. 2 to points all the way across the charge. For $\ell \leq 12.7$ cm, Eq. 1 has also been used in the same manner, the results being reported in column 6. For these data, there is little difference between the results obtained from the two equations. Because the AP charges very rapidly develop a constant R_c, in the following discussions we will only refer to the results obtained from Eq. 2 (col. 5); these are plotted in Fig. 7. Discussion of this figure will be more understandable if we first review briefly some of our general knowledge of shock-to-detonation transition.

The shock initiation of detonation depends upon the area of shock front in the acceptor as well as the pressure-time history which that shocked area experiences. According to the particular combination of these factors, the detonation induced in the acceptor may be temporarily under or overdriven. In the first case, the shock induced reaction is highly exothermic but is sub-detonation. Consequently, the energy of reaction exceeds the energy lost by any dissipative processes until the reaction has built up to its steady state. In the case of overdrive, a strong shock initiates reaction at a higher temperature and pressure than the steady state C-J values. Consequently, the excess energy is dissipated until the steady state condition is reached. Overdrive (or underdrive) decreases to a negligible amount by the time the disturbance has travelled to $(\ell/d) = 2$ even when the donor and acceptor are badly mismatched.[13]

The data of Table 4 show that, for AP, R_c decreases to the constant value each attains at $(\ell/d) \geq 1.5$. A similar decrease in D can be detected at the lowest density. Thus our initiation system of a detonator followed by a 25.4 mm long

pentolite booster overdrives the AP detonation, and the overdrive increases with increasing particle size. The detonation front in AP does not exhibit a spherical expansion, but rapidly attains constant R_c, a behavior reported by Cook[2] for non-ideal explosives. At small values of ℓ, however, the Ref. (2) curves followed the spherical expansion line, i.e., detonator initiation* (approximately, point initiation) resulted in an underdriven detonation which built up to the steady state.

It is concluded from the constant plateau values found in each case that plane wave propagation of steady-state detonation in AP is impossible in 50 mm diam. charges. Thus a plane wave booster would be expected to affect the wave shape only in the transitional region in which the over boostering is fading out. This was confirmed by shots 772 and 773 in which ca. 9 μ AP (N140) at ρ_o = 1.29 g/cc was initiated with a PWB. At (ℓ/d) of 1.0 and 2.0, the R_c values were 61 and 66 mm, respectively. The latter value falls on Fig. 7 about where it should for 9 μ AP, i.e., linear interpolation on the density to 1.29 g/cc gives an R_c value for AP (N138) of 65 mm. Thus the plateau region of Fig. 7 seems independent of the original source of initiation. Hence there is no point to initiating AP with a PWB for the electromagnetic studies. On the other hand, it seems safe to assume that constant D and R_c will have been attained at (ℓ/d) = 1.5 instead of only at (ℓ/d) $\geq$ 3.0 as we have been assuming. For steady state values then, we can use shorter charges than we had thought necessary.

In the corrections we have recently used on our detonation velocity measurements, we assumed: (1) spherical expansion of the detonation front and (2) an

* Where a booster was necessary, the detonator was placed in a 19 mm deep well in a 25.4 mm booster.[14] Unfortunately, Cook did not indicate whether his coarse TNT and TNT/$NaNO_3$ mix were cap sensitive or not. If not, the detonator would still have been only 6.4 mm from the main charge surface and hence approximated point initiation better than the initiator of the present work.

increase in R_c as detonation passed from the booster (donor) to the main AP charge (acceptor). Fig 7 shows that both of these assumptions are wrong for AP. For this explosive, the uncorrected velocity (measured optically or with pins along the charge surface) is also the axial velocity.

Finally, several non-detonating charges (fading reaction) were examined. These data in Table 5 show no obvious change in R_c with failure to detonate; the x-y data can be fitted to Eq. 1 or Eq. 2 as well as those from detonating charges. However, the luminosity of the trace shows interesting changes with charge length. At ℓ = 25.4 mm or (ℓ/d) = 0.5, the effect of the booster is dominant here as it is for the detonating charges. R_c is 71 mm (Shot 754) as compared to 72-74 mm in Fig. 7. In other words, at (ℓ/d) = 0.5, R_c is the same regardless of particle size, loading density, and whether the disturbance is a strong shock or a true detonation. At (ℓ/d) = 1.5 for the 26 μ AP at ρ_o = 1.435, R_c is still in the range of the Fig. 7 curves and the wave profile in AP at this density and particle size has faded out at both edges (See Fig. 2, Shot 731) so that only 0.9 d is covered. An even better example of the progress of fading of the reaction from the surface of the charge to its central axis is shown by this AP at ρ_o = 1.40 - 1.41 g/cc. This density is nearer the failure point (ca. 1.385 g/cc, see Fig. 4) and consequently the failing reaction persists longer. At (ℓ/d) = 3, the wave profile still covers the diameter, but by (ℓ/d) = 3.5 only a very faint trace can be seen which covers just the central third of the diameter.

NQ

The second explosive studied was low bulk density nitroguanidine, NQ-ℓ, X547. This was studied at 56% and 92% TMD rather than at 60 and 69% TMD as was the case for AP.[7] This greater spread in density may make the results differ significantly from those for the AP. Data on results for both densities of NQ-ℓ are given in

Table 6; the radii of curvature are shown in Fig. 8. Eq. 1 was used to fit the data for the high density charges, Eq. 2 for the low density charges*. In other words, the shock from the 1.65 g/cc material seems to expand more nearly radially than does the 1.0 g/cc material. The solid diagonal line in Fig. 8 represents simple radial expansion with no regard for the booster charge. Hence it is not surprising that the point for ℓ = 76.2 mm lies above the solid line. The dashed curve passes through two points as a straight line and extrapolates to an effective initiator length of 22 mm (i.e., ℓ = -22.0 for R_c = 0), which is close to the 25.4 mm booster length. This is reasonable since the pentolite booster and the higher density NQ have nearly the same impedance. Radial expansion apparently breaks down somewhere between ℓ = 127 and 229 mm, or between (ℓ/d) = 2.5 and 4.5. If the actual booster length is added to the length of the charge, we have breakdown between 3.0 and 5.0 for ℓ'/d', $\ell' = \ell + 25.4$ mm. These numbers are more suggestive than accurate. For example, note the error bars which have been placed on the points for ρ_o = 1.65 g/cc. These errors are based on one standard deviation of the computed value of the quantity R_c in Eq. 1. Obviously we need more data before we can be certain about the behavior of this material.

The behavior of NQ-ℓ at a density of 1.0 g/cc is much more similar to that of AP. Equation 2 was used to fit these data and the results are shown in Fig.8 also. We find a constant value of R_c of 94 mm beyond ℓ = 76.2 mm. Hence this material has a constant R_c for (ℓ/d) $\geq$ 1.5. As in the case of the AP, this material is possibly overboostered. Since our data show only the constant value of R_c, the estimate of effective initiator length (18 mm) can be only a lower limit

* Data of Table 6 show that fitting the data for 1.65 g/cc with Eq. 2 gives a trend of R_c vs ℓ/d that cannot be readily interpreted. The use of Eq. 1, however, leads to the interpretation of the text.

approximation. Again, more data are needed to clarify the situation completely. We have, however, enough data to guide us in future work on 1.0 g/cc density charges of NQ-ℓ in the electromagnetic experiments.

It is evident that for NQ-ℓ, R_c increases as ρ_o increases, the same trend as that reported for ideal explosives by Cook[2] and the reverse of the trend found for AP. The trend with density indicates that NQ-ℓ at ρ_o = 0.4 g/cc will have $R_c < 94$ mm and constant R_c at $(\ell/d) \geq 1.5$. Hence the successful use of such low density NQ in a plane wave generator[15] must have resulted from overboostering the NQ.

TNT, ρ_o = 1.081 g/cc.

Because NQ seems, in some ways, an atypical organic H.E., radius of curvature measurements were also carried out on low density TNT, X517. The data are given in Table 7. Although the scatter in R_c is large, this would be expected because of three difficulties in controlling charge preparation. These are large particle size (ca. 200 μ), low charge density ($\sim$1.0 g/cc), and compaction in the hydraulic press, all factors which favor local irregularities in the charge. With allowance for the larger scatter, it seems clear that low density TNT behaves like AP, i.e., has a constant R_c at $(\ell/d) \geq 1.5$.

Pressed RDX

The lowest density charges of RDX which could be prepared in the isostatic press were those at about 1.3 g/cc. This material, X659, is fine grained and the charges were expected to be of good quality. That is, isostatic pressing of a fine, chemically homogeneous material usually results in uniform charges as was true in this case. Data for the experiments are given in Table 8; these are for detonation velocity in RDX at ρ_o = 1.3 g/cc and for curvature studies in both boostered charges of RDX and detonator initiated charges. Equation 1 was applied to data

from these shots and the resulting values of R_c are shown in Fig. 9. Again the error bars are given by the computer program which fits the data -- we have not analyzed the situation for experimental errors, biased or unbiased. Although the quality of the charges was excellent, the errors are surprisingly large for both boostered and detonator initiated charges. For both sets of data, we have omitted from the graph the value of R_c for ℓ = 25.4 mm. This was done because we are not sure that the detonation velocity has reached a steady state at this distance -- even for the boostered charge. If the velocity is not constant, our method of analysis breaks down -- see the derivations of Eq. 1 and 2.*

Discarding the data for ℓ = 25.4 mm leaves only 2 points to establish a line for radial expansion of the detonator initiated charges. This extrapolates to an effective initiator length of 33 mm for RDX (ρ_o = 1.3 g/cc). That is, the front appeared to have started 33 mm behind the charge. Certainly more data on curvature and on detonation velocity are needed in this case. We can hazard a guess that the front is expanding radially out to ℓ/d of at least 4.5.

The results for pentolite boostered charges of RDX (ρ_o = 1.3 g/cc) are also shown in Fig. 9. These were obtained by using Eq. 1 (assuming radial expansion); errors being estimated as outlined above. A straight line (— - — -) fits these results fairly well, but it gives an effective initiator length of 63 mm. Subtracting the 33 mm obtained above from the 63 mm effective initiator length, we have 30 mm length of RDX (1.3 g/cc) equivalent to 25.4 mm pentolite (1.56 g/cc). Inasmuch as the ratio of the impedances (pentolite/RDX) is 1.21, this seems a reasonable equivalence. Apparently we do not have enough information on the

* The two points at ℓ = 25.4 mm [(ℓ/d) = 0.5] fall well below the curves of Fig. 9. The measured front velocity at this location (see Table 8) supports the suggestion that the steady state velocity had not yet been achieved. It is also relevant to note that the initiator effect is still dominant at this low value of (ℓ/d) for AP. (See Fig. 7).

boostered system or on the detonator initiated system. We have, however, enough information on both systems so that we can design electromagnetic experiments for measuring particle velocity with some assurance as to the amount of curvature to expect in the detonation front. That is, the front in RDX (1.3 g/cc) expands radially out to at least $(\ell/d) \sim 4.5$. This does not agree with the behavior reported for 1.2 g/cc RDX in Fig 5.7a of Ref. 2. The difference might arise from the density difference (1.2 g/cc vs 1.3 g/cc); from a difference in particle size; or from a difference in data analysis.

Tetryl

The curvature of the detonation front in tetryl charges has been reported previously[1]. A 35 mm streak camera was used in that work so that resolution of both time and distance was not as good as with the 70 mm camera now used. One consequence of this is that the data near the center of the charge were of low significance. Thus the fit to Eq. 1 was governed mostly by the data over the last 1.2 cm on each edge of the charge, and the requirement that the curve pass through the points $t = 0$, $x = 0$. These data have been re-examined; they were fitted to both Eqs. 1 and 2. The main change is that the results for the 200 mm long charges now lie close to the radial expansion line rather than above it, see Fig. 10. This is probably due to an improvement in the computer code. Plotting the experimental data and the values computed from the new fit clearly demonstrate that the new fit is superior for a 200 mm long charge. Tetryl ($\rho_0 = 1.51$ g/cc) exhibits radial expansion out to 200 mm, $(\ell/d) = 4$, as stated previously.

Summary R_c vs ℓ Fig. 11 summarizes the R_c vs ℓ measurements we have made and reported. Though by no means a complete survey, it strongly indicates that any low density ($\rho_0 \sim 1.0$ g/cc) explosive will rapidly attain a constant R_c at $(\ell/d) \geq 1.5$ whether the explosive is ideal or non-ideal. High density conventional explosives, e.g., tetryl at 87% TMD, exhibit a geometrical spherical expansion of

the detonation front at $\ell/d \leq 4.0$. There may be cases intermediate between these two extremes, e.g., NQ at 92% TMD. In addition to ρ_o, R_c depends on the nature of the material and on its particle size.

Estimates of Reaction Zone Length

The Wood and Kirkwood curved front theory[4] derives the relationship

$$z = (s/3.5)(1-D/D_i) \qquad (4)$$

where z is the reaction zone length, s is the radius of curvature R_c, and the numeric factor is somewhat arbitrary. For H.E. showing constant s at $(\ell/d) \geq 1.5$, z can be computed from our present data although the results for NQ and TNT will be only approximate. For expanding fronts, if we assume z constant, then s and D must change together. Computation of z then requires at least a pair of (s,D) values; many pairs would be preferable. Good derived z values for tetryl, and for RDX cannot be obtained without much more precise measurement of both D and R_c vs ℓ, but an estimate of the size of z can be made.

Table 9 contains the results, and the z values for the two APs are plotted in Fig. 12a; Fig. 12b shows the "a" values computed from the original curved front theory[5] and reported for two different particle size APs in previous work[6]. Fig. 12a shows first that the density has only a small absolute effect on the z value. For the 25 μ AP, whatever that effect is, it is submerged in the general scatter of the results. In the case of the 9 μ AP, the trend is quite smooth: z decreases with increasing ρ_o to a minimum at 1.2 g/cc after which it increases again. The minimum occurs at about the density where the D vs ρ_o curve departs from linearity (see Fig. 4). The z value for the finer material is less than that for the coarser, but the ratio value is 0.24 to 0.19 whereas the δ ratio of 9/25 is 0.36. Hence the ratio of these nominal reaction zone lengths, z, does not equal the ratio of the average particle sizes as did the ratio of the nominal zone lengths a [6].

In Fig. 12b, from a previous report[6], both the 25 μ and the 10 μ material show a vs ρ_o curves at $\rho_o \leq 1.0$ g/cc very similar to the z vs ρ_o curve of the fine AP in Fig. 12a. Since the earlier work was done, we have found[12] that for AP at $\rho_o > 1$ g/cc our diameter series, terminating at d = 7.6 cm, is inadequate for extrapolation to D_i values; in particular, the slope of the D vs d^{-1} curve is too steep. (Also see Appendix) Because "a" is directly proportional to that slope, the a values at $\rho_o > 1.0$ g/cc in Fig. 12b are all too high, and because the error increases with the density, it is probably responsible for the sharp increase in "a" indicated at higher ρ_o in Fig. 12b. In the region where this error does not occur, i.e., $\rho_o < 1.0$ g/cc, the a/z ratio for the 25 μ AP (N126 in both cases) is about 3.0. The 9 μ AP value of z can be approximately adjusted to that for 10 μ by assuming proportionality between z and δ. Then the a/z ratio for 10 μ AP is 3.9. For AP at low ρ_o, the a/z ratio seems to be appreciably less than the value of 7 reported for conventional H.E.[17].

The value of z for the 9 μ AP at 1.3 g/cc (1.10 mm) is quite close to a preliminary measurement of the zone by the electro-magnetic method (1.1 to 1.7 mm at 1.29 g/cc). The z value for low ρ_o TNT compares fairly well with measurements[18] (1.2 vs 1.6 mm) but that for moderate ρ_o RDX does not (0.2 mm vs 0.6 to 0.9 mm). In both these cases, however, the agreement or disagreement could result from very small errors in the value of D used. For example, Table 8 lists three acceptable experimental values of D for RDX; each is within 0.6% of D_i. For spherical expansion of the detonation front, R_c and D are both assumed to increase with (ℓ/d) until ideal values (∞ and D_i) are reached. Hence the two values of $D < D_i$ of Table 8 were chosen to compute z (Table 9); the apparent agreement for the two results is probably fortuitous and depends on the difference of 0.02 mm/μsec in D which is well below our experimental resolution. Future work will include additional investigation of experimental measurement and methods of computation of reaction zone lengths.

SUMMARY AND CONCLUSIONS

The present study of curvature of the detonation front was carried out at constant diameter ($\sim$50 mm). Hence no information on the effect of d on R_c was obtained although d is considered one of the variables which determine R_c. Information obtained in the study follows:

1. Non-planar detonation fronts are well approximated by a spherical shape; edge effects are small.
2. R_c is a function of the chemical material, its particle size δ, and its ρ_o. R_c increases with decreasing δ. R_c may increase with increasing ρ_o (e.g., NQ) or decrease with increasing ρ_o (e.g., AP). The effect of ρ_o may be associated with Group 1 or Group 2 classification.
3. Any charge having $\rho_o \leq 1.0$ g/cc appears to have a constant R_c, rapidly attained, and independent of the type of initiation. For point initiation, constant R_c is established at $(\ell/d) \geq 1.5$.
4. AP exhibits rapidly attained constant curvature of the detonation front over the density range in which it is detonable, whereas tetryl (and presumably other conventional H.E.) at high ρ_o ($\geq$87% TMD) exhibits a geometrical spherical expansion with ℓ/d.
5. NQ may be excluded from "conventional" H.E. since at 92% TMD it appears to exhibit a behavior intermediate between that of AP and that of tetryl at 87% TMD.
6. From the standpoint of failure theory, the behavior of subcritical charges is of much interest. Strongly boostered, subcritical charges show failure starting with quenching of the reaction at

the charge surface and working toward the axis. There is no marked increase in R_c during this process, nor does R_c seem to decrease to 0.5 d at $d = d_c$.

7. The method of correcting our measured D values[3] is not applicable to any charge at $\rho_o \sim 1.0$ g/cc or to any charge of AP. It does seem to be applicable to most high density organic H.E. although it is only partially so to NQ at 92% TMD. Consequently we can use this correction only in the special cases where we know or have shown by test that it is valid.

8. In the electromagnetic measurement of particle velocity a plane wave booster cannot produce a steady state planar detonation in AP charges or (probably) any other charges of $\rho_o \sim 1.0$ g/cc. For these charges, the constant D and R_c will be established at $(\ell/d) \geq 1.5$. (We have previously assumed that $(\ell/d) \geq 3$ is necessary).

REFERENCES

1. I. Jaffe and A. R. Clairmont, "The Effects of Configuration and Confinement on Booster Characteristics", NOLTR 65-33 (13 Apr 1965).

2. M. A. Cook, "The Science of High Explosives", Reinhold Pub. Corp., New York (1958), pp 99-104.

3. J. O. Erkman, "Velocity of Detonation from Streak Camera Records", NOLTR 68-117 (19 Sep 1968).

4. W. W. Wood and J. G. Kirkwood, J. Chem. Phys. 22, 1920(1954).

5. H. Eyring, R. E. Powell, G. H. Duffey and R. B. Parlin, Chem. Revs. 45, 69-181 (1949).

6. D. Price, A. R. Clairmont, Jr. and I. Jaffe, "Particle Size Effect on Explosive Behavior of Ammonium Perchlorate", NOLTR 67-112 (27 Sep 1967).

7. D. Price and A. R. Clairmont, Jr., "The Response of Nitroguanidine to a Strong Shock", NOLTR 67-169 (2 Feb 1968).

8. D. Price, A. R. Clairmont, Jr., and I. Jaffe, Combustion and Flame 11, 415-25(1967).

9. D. Price, I. Jaffe, and J. P. Toscano, NOLTR 66-21 (17 Mar 1966), pp 3-4.

10. A. R. Clairmont and I. Jaffe, NOLTR 64-23 (16 Mar 1964).

11. I. Jaffe, J. Toscano, and D. Price, NOLTR 64-66, Appendix II (2 Jul 1964)

12. D. Price, A. R. Clairmont, Jr., J. O. Erkman, and D. J. Edwards, NOLTR 68-182 (16 Dec 1968).

13. L. C. Smith, Explosivstoffe 5 (1967), p 110.

14. M. A. Cook, G. S. Horsley, R. T. Keyes, W. S. Partridge, and W. O. Ursenbach, J. Appl. Phys. 27, 269(1956).

15. W. B. Benedick, Rev. Sci. Instru. 36, 1309 (1965).

16. Properties of Chemical Explosives, UCRL-14592, Univ. Cal., LRL, Livermore, Cal. (1965).

17. L. G. Green and E. James, Jr., "Radius of Curvature Effect on Detonation Velocity", Fourth Symposium (International) on Detonation, ACR-126, Govt. Print. Office, Washington, D.C. (1967) pp 86-91.

18. A. N. Dremin and K. K. Shvedov, Zh. Prikl. Mekh. Tekh. Fiz. No. 2, 154(1964).

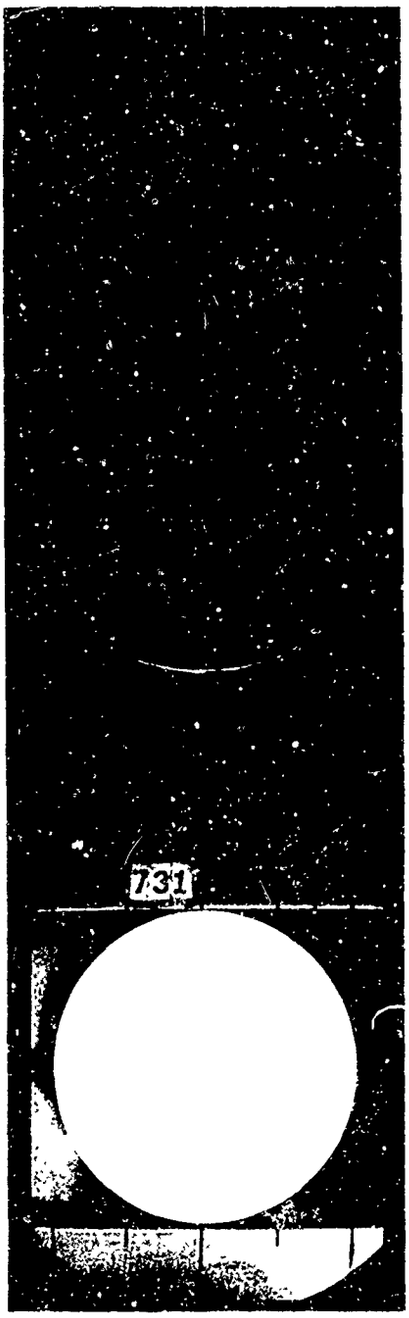

(a) SHOT 731: 25μ AP (N126), ρ_o = 1.435i, ℓ = 114 mm.

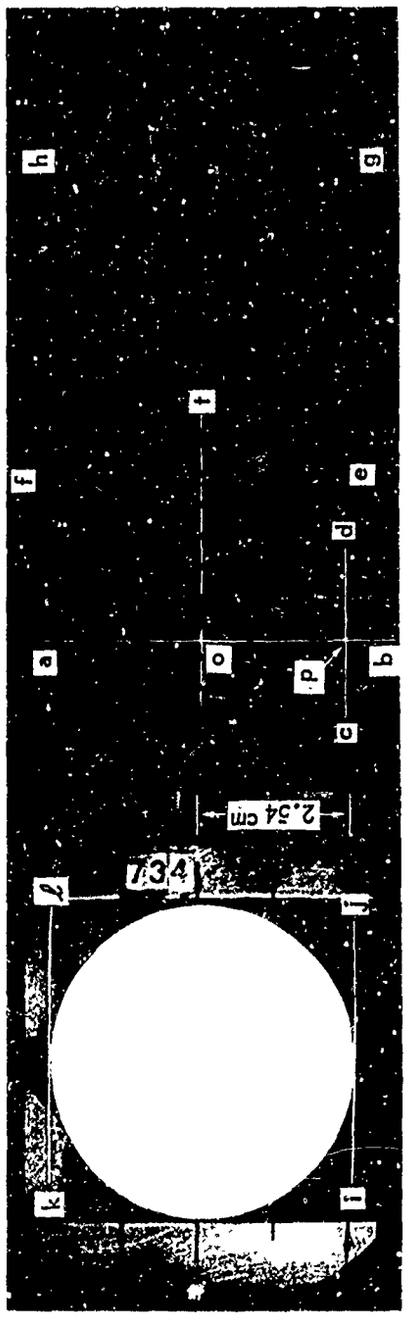

(b) SHOT 734: 9μ AP (N138), ρ_o = 1.021H, ℓ = 239 mm.

FIG. 1 TYPICAL SMEAR CAMERA RECORDS OF CURVED DETONATION FRONT.(TIME INCREASES TO RIGHT.)

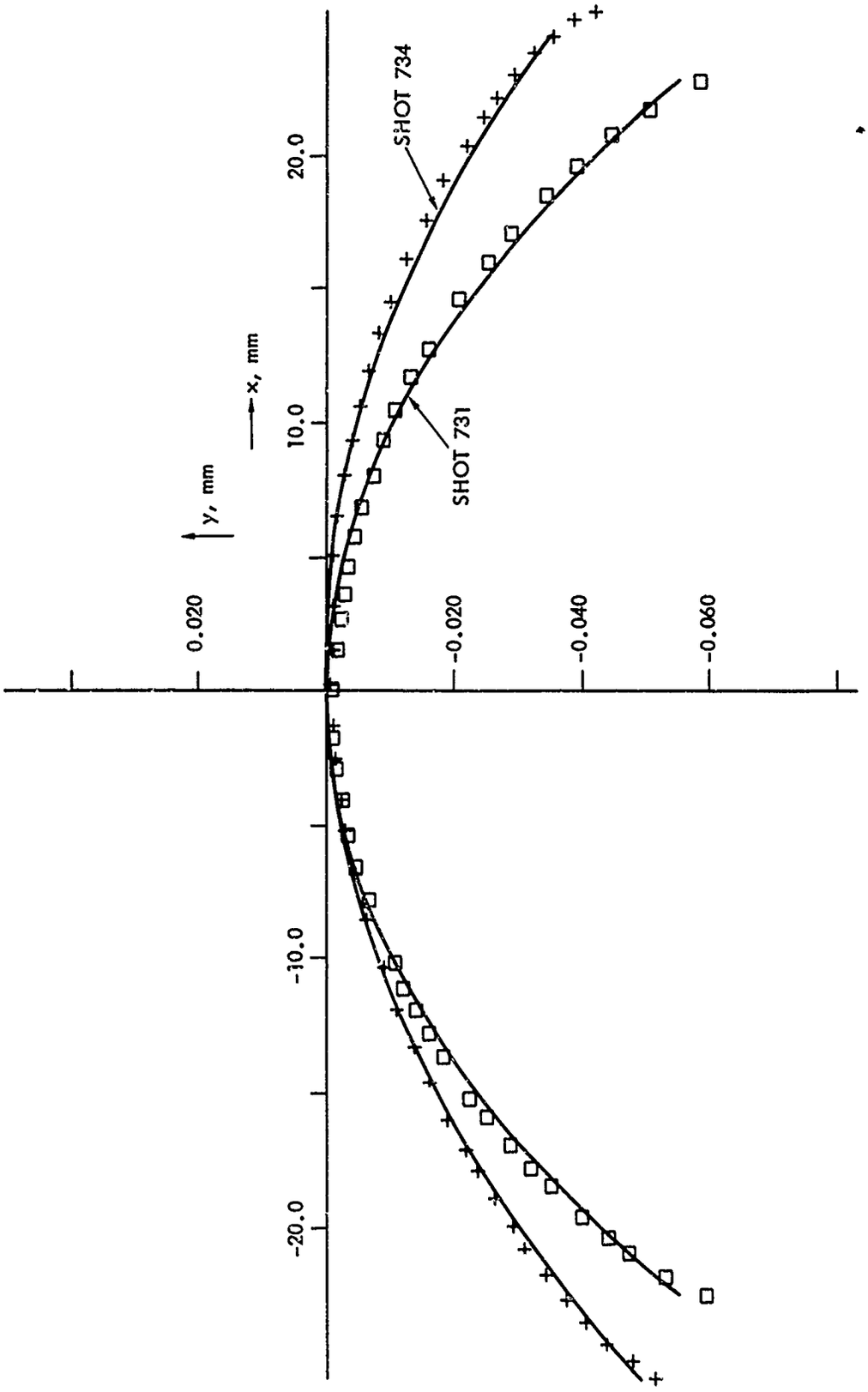

FIG. 2 SMOOTHED (x,y) DATA FROM RECORDS SHOWN IN FIG. 1

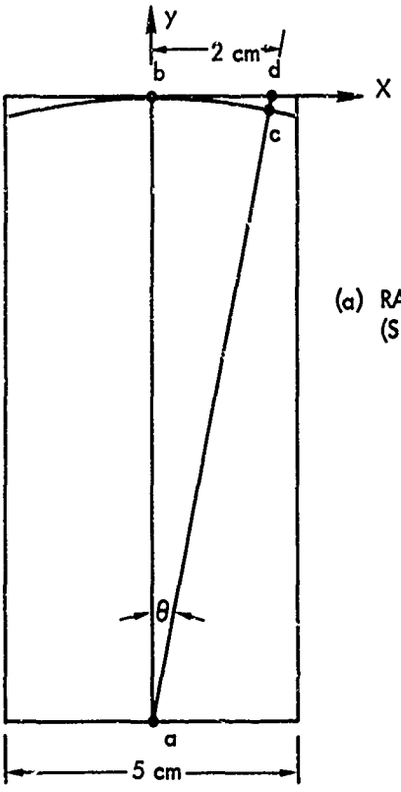

(a) RADIAL EXPANSION
(SEE EQ. 1)

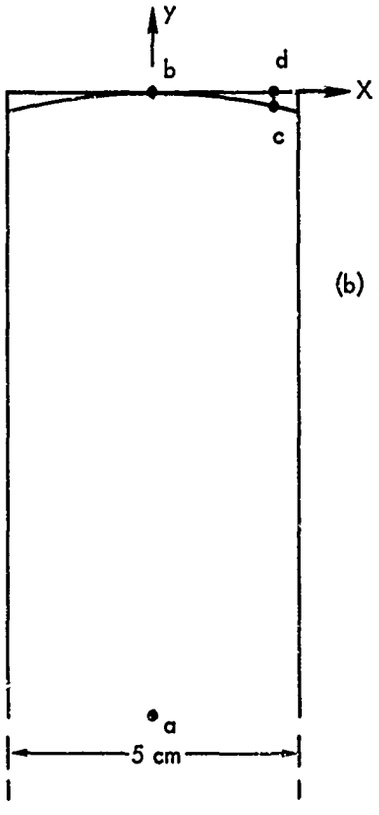

(b) STEADY CURVED FRONT
(SEE EQ. 2)

FIG. 3 TWO MODELS FOR EXPANSION OF DETONATION FRONT IN CYLINDRICAL CHARGE.

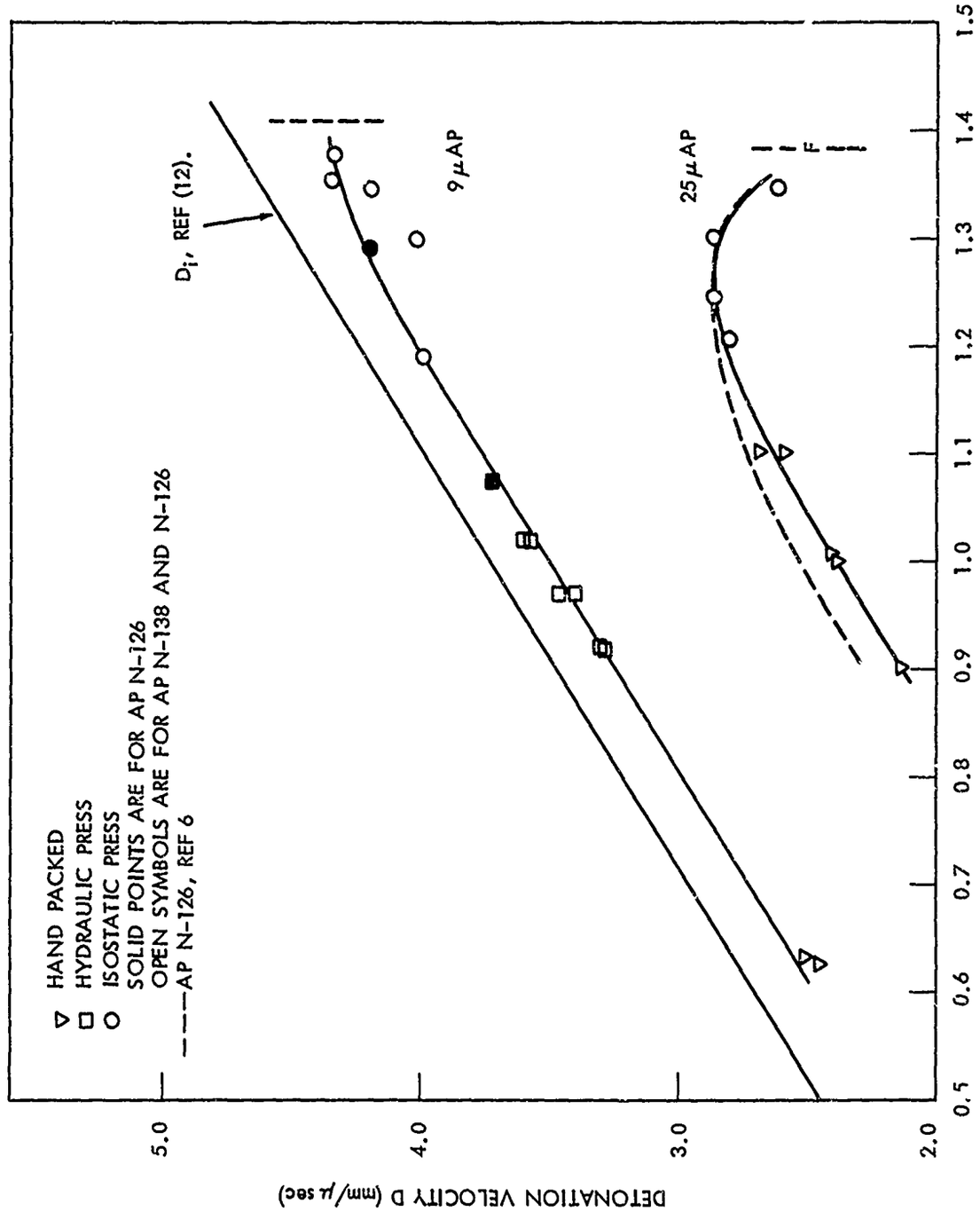

FIG. 4 D VS ρ_o CURVES FOR 9 μ AND 25 μ AP AT d ~ 50 mm.

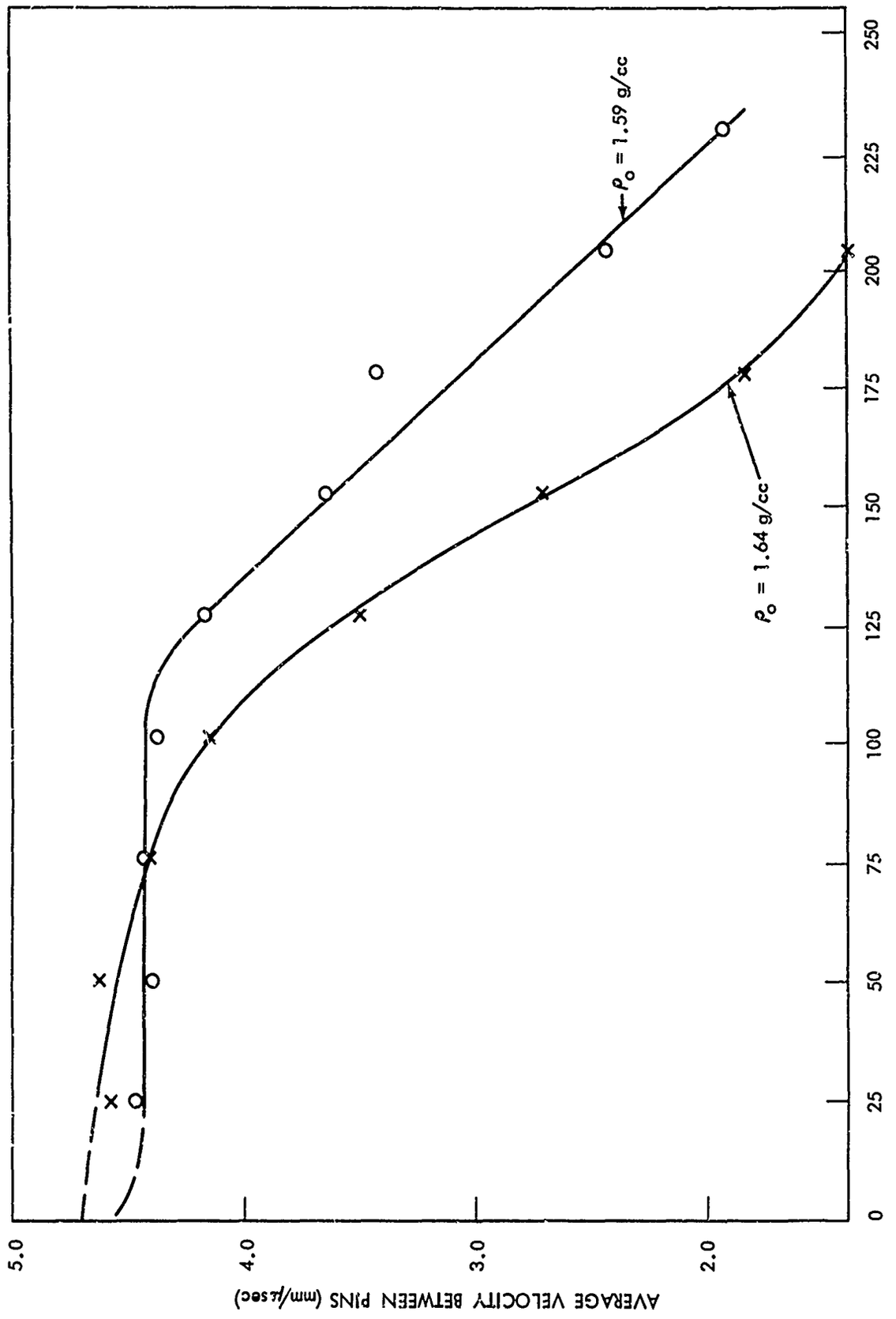

FIG. 5 FAILING REACTIONS OF 9μ AP (N138) IN GAP TEST CONFINEMENT.

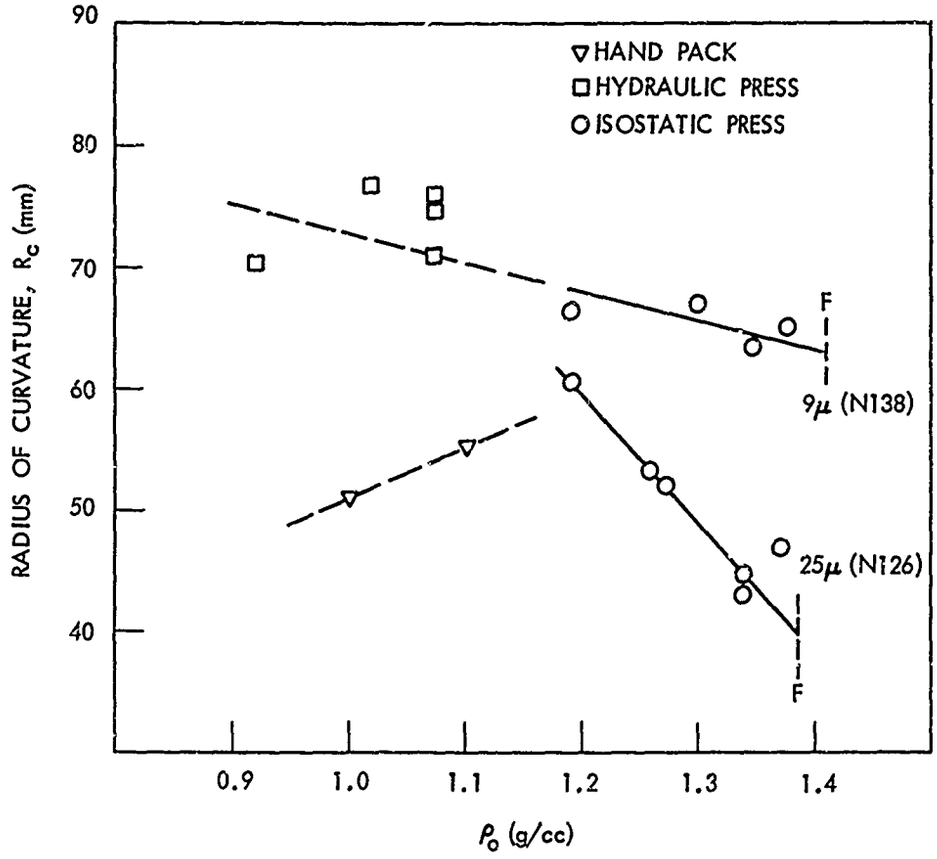

FIG. 6 R_c VS ρ_o CURVES FOR 9μ AND 25μ AP AT d~50mm.

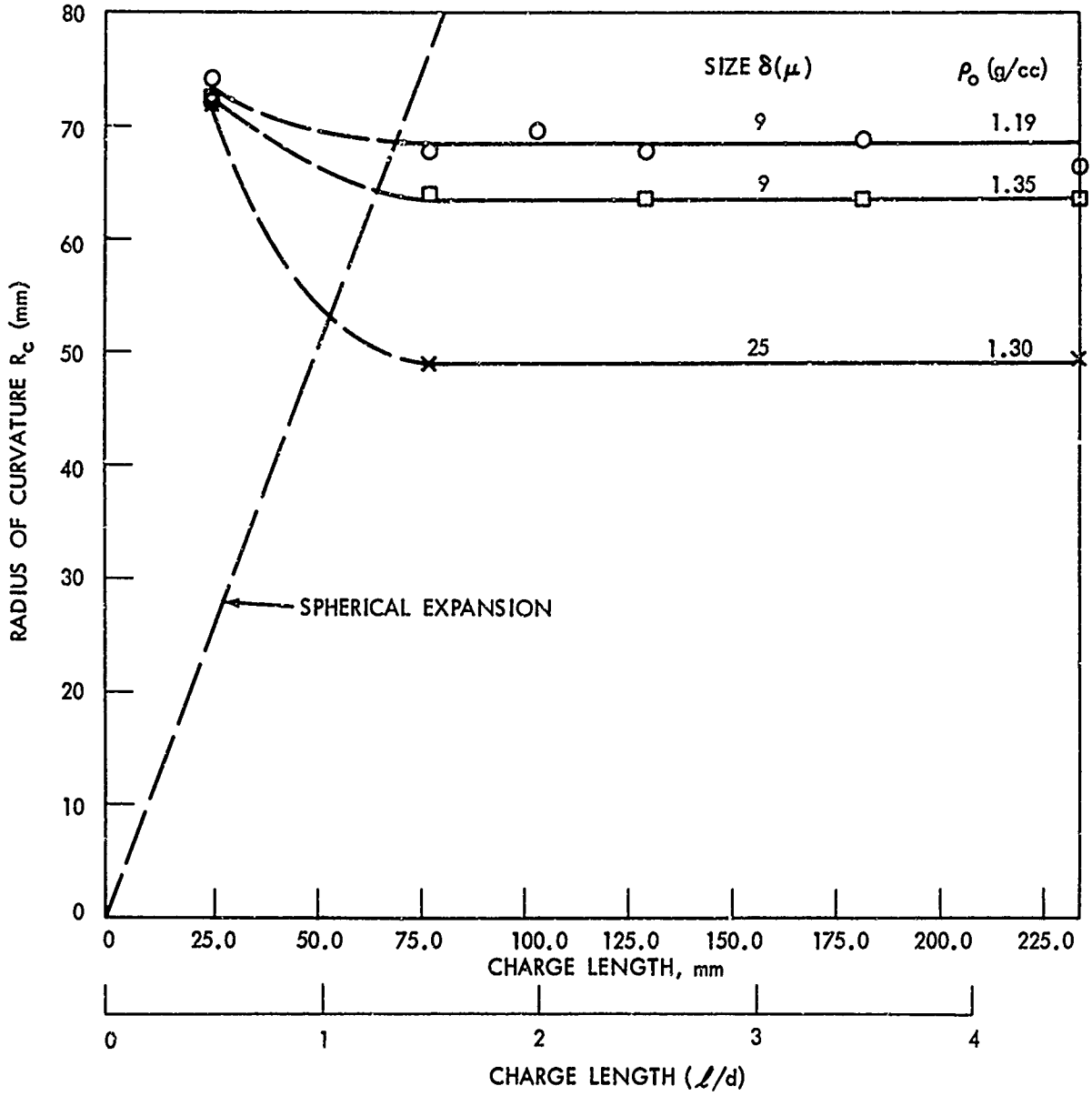

FIG. 7 RADIUS OF CURVATURE VS LENGTH OF AP CHARGES OF N-138 AND N-126, d = 50.8mm

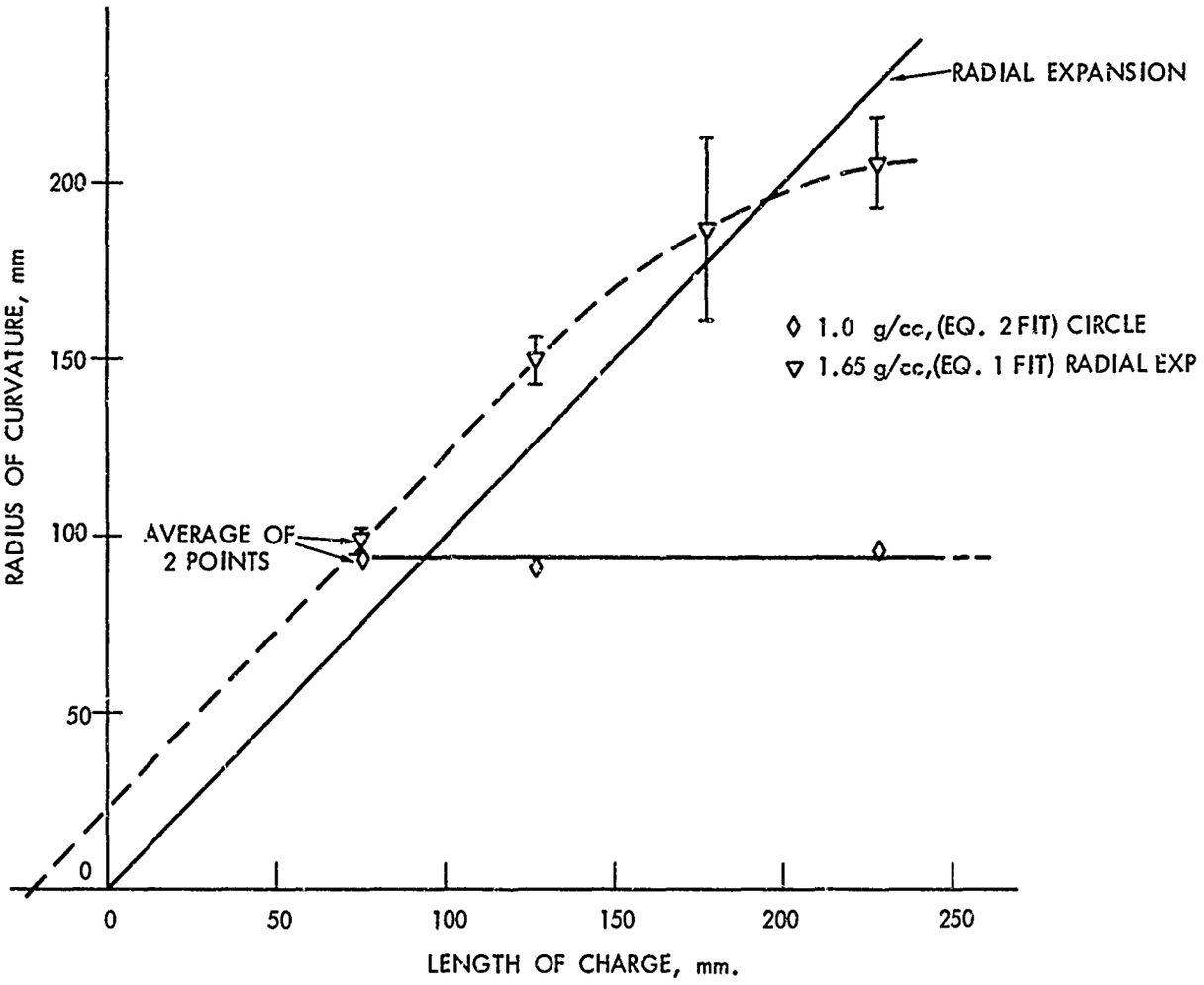

FIG. 8 R_c VS LENGTH OF CHARGES OF NQ - ℓ, (X547).

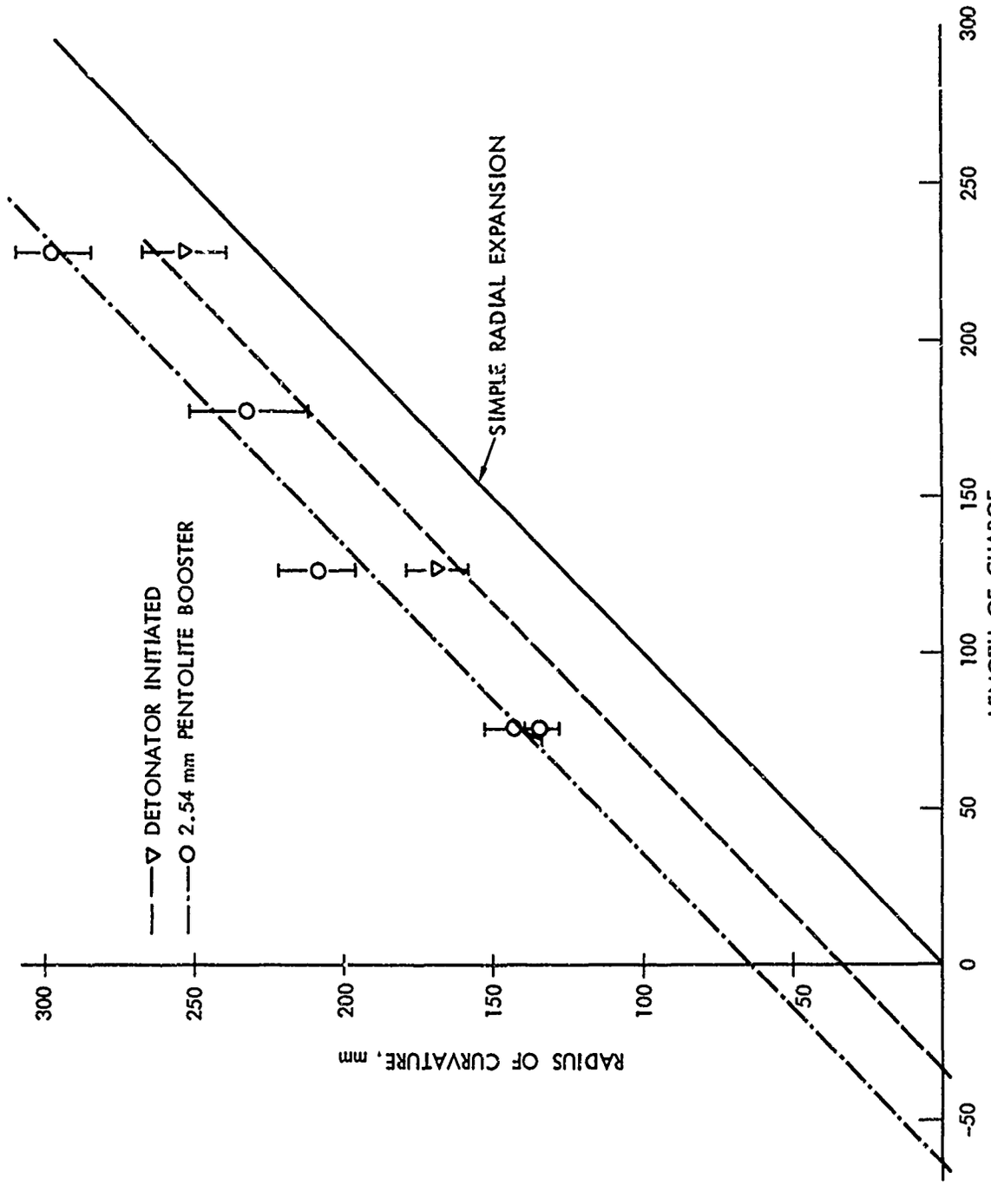

FIG. 9 R_c VS LENGTH OF RDX (X659) CHARGES, (ρ_o = 1.3 g/cc, d=50.8 mm,) FITTED BY EQ. 1.

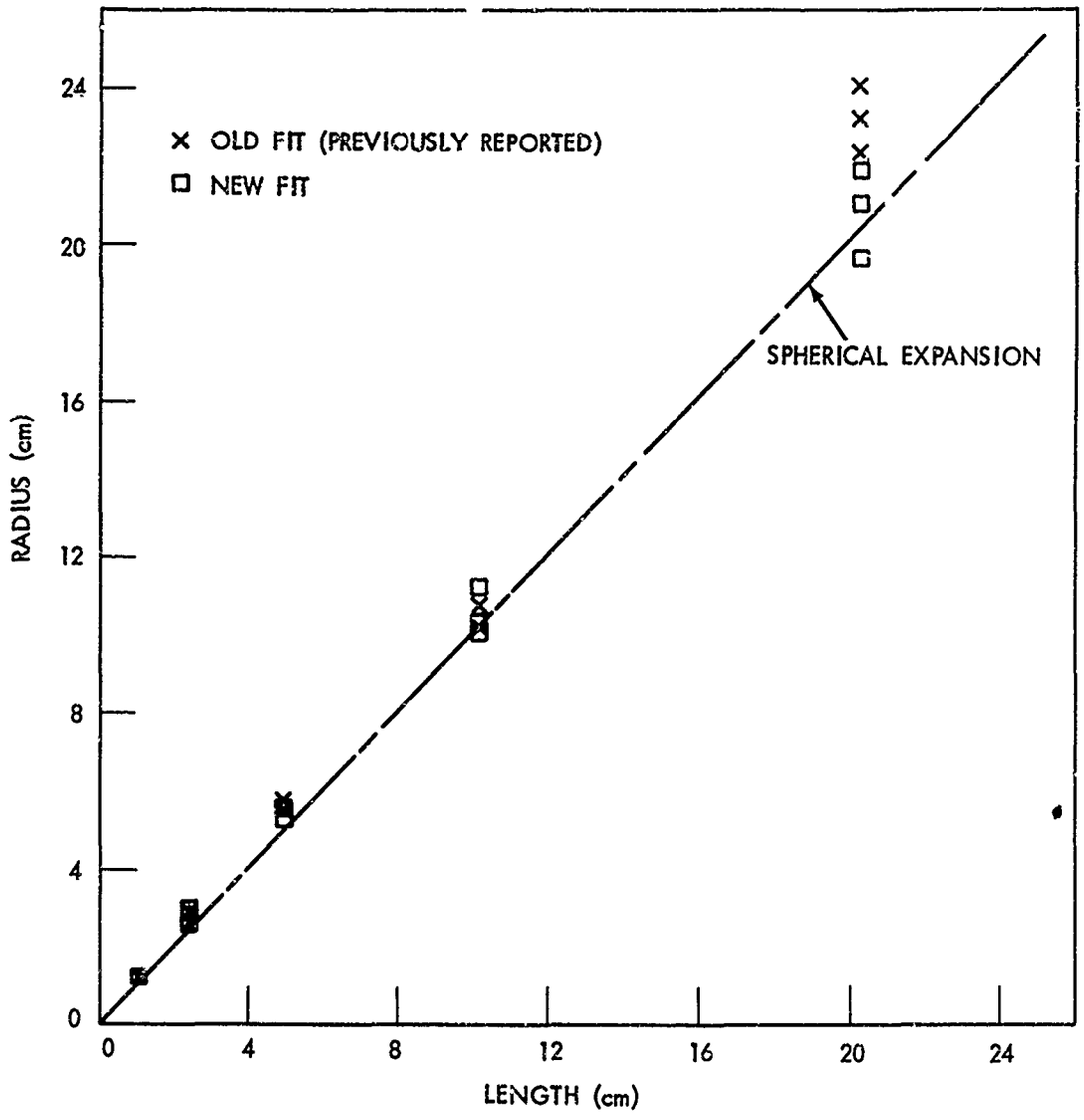

FIG. 10 R_c VS LENGTH OF TETRYL CHARGES, d = 50.8 mm

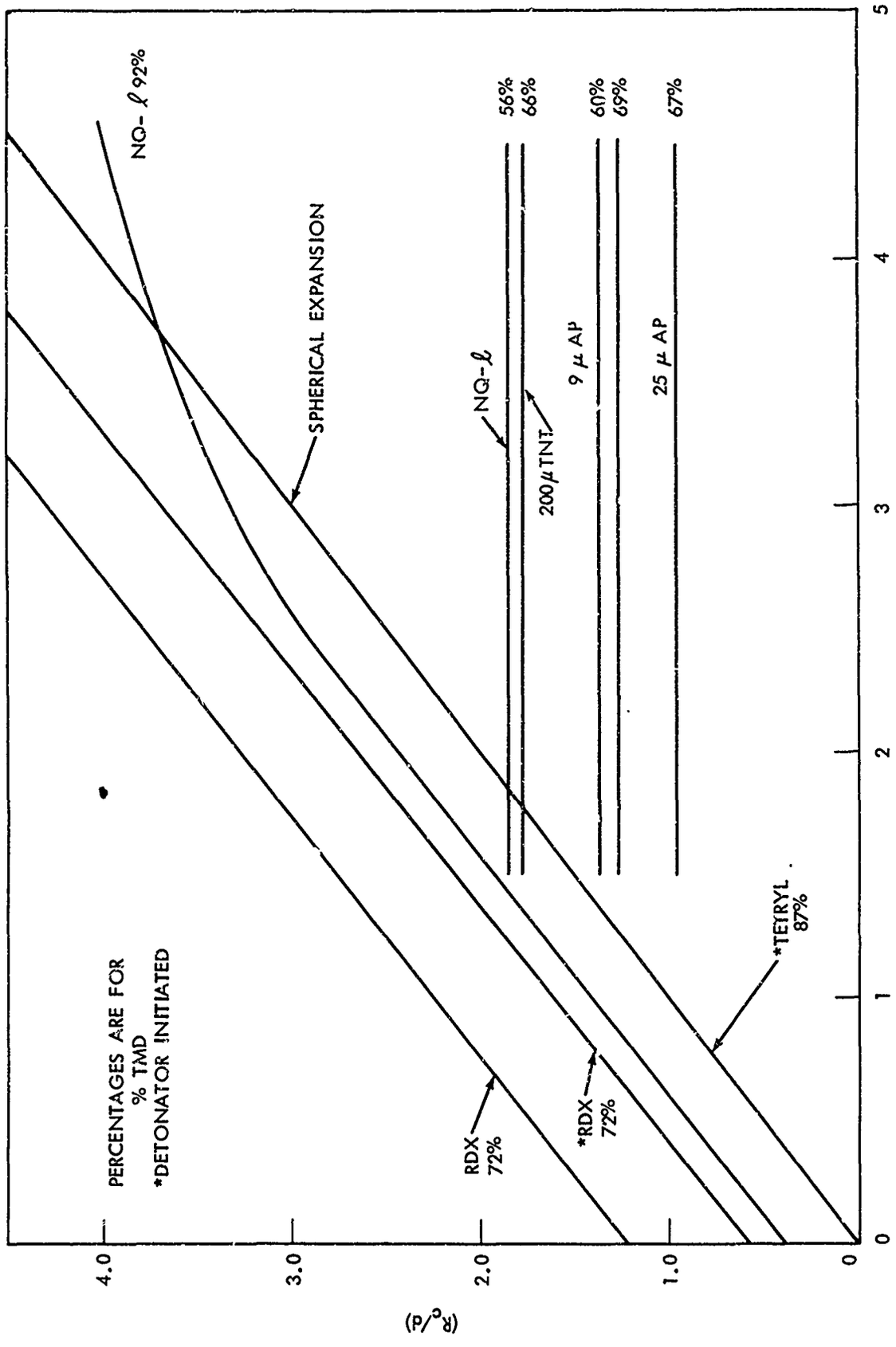

FIG. 11 SUMMARY OF NOL RADIUS OF CURVATURE VS CHARGE LENGTH MEASUREMENTS.

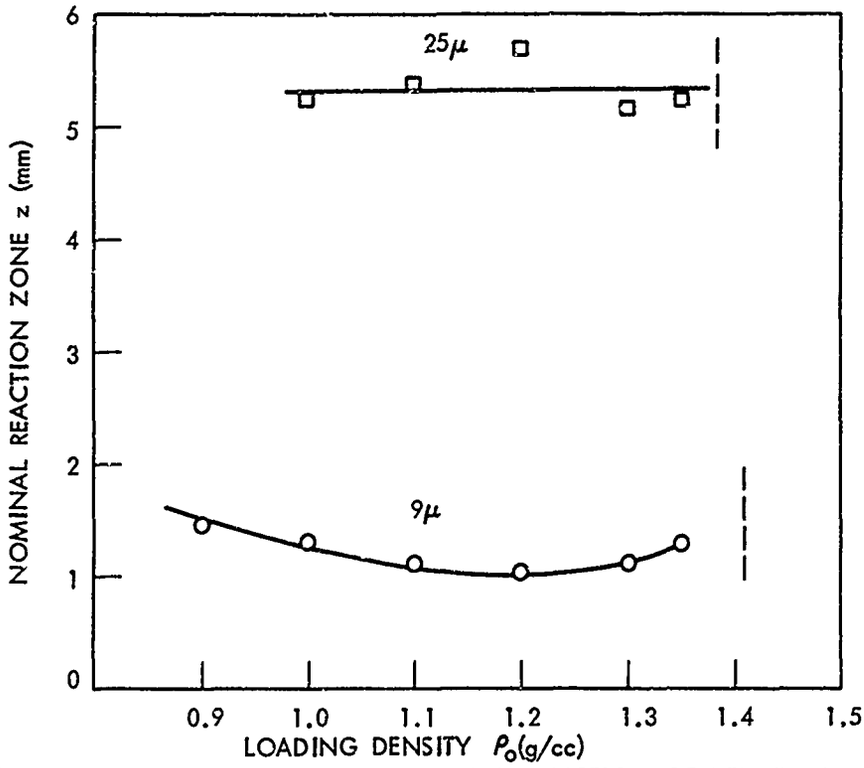

(a) NOMINAL REACTION ZONE LENGTHS, z, FOR AP AS A FUNCTION OF DENSITY & PARTICLE SIZE

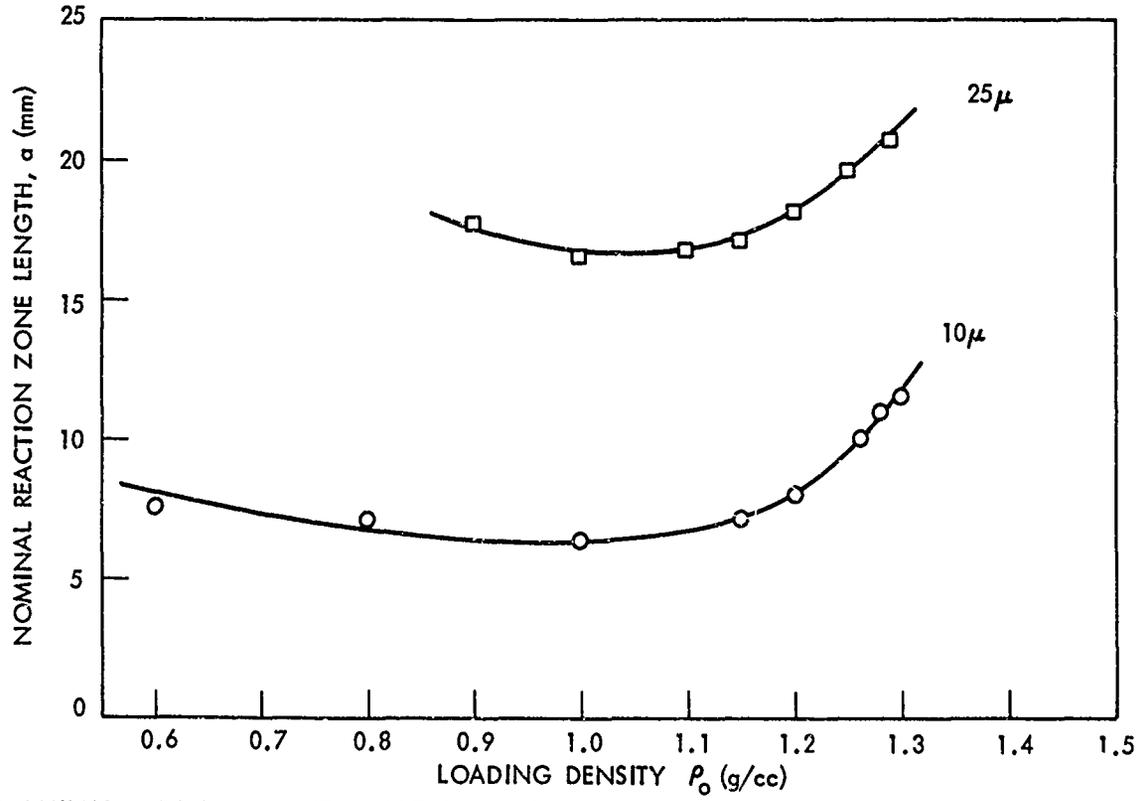

(b) NOMINAL REACTION ZONE LENGTHS, a, FOR AP AS A FUNCTION OF DENSITY & PARTICLE SIZE

FIG. 12 NOMINAL REACTION ZONE LENGTHS FOR AP AS A FUNCTION OF DENSITY AND PARTICLE SIZE.

Table 1

DETONATION VELOCITY DATA FOR AP's

Shot No.	ρ_o (g/cc)	d (mm)	D (mm/μsec)	Comment
	AP(N138) 8.9μ			
651	0.627h	50.8	2.452	
654	0.633h	50.8	2.502	
704-1	0.920H	50.6[a]	3.286	
705-1	0.920H	50.6[a]	3.302	
706-1	0.970H	50.6[a]	3.459	
710-1	0.970H	50.6[a]	3.394	
652	1.020H	50.3	3.558	
655	1.020H	50.3	3.590	
697	1.190i	49.9	3.985	
698	1.299i	49.9	4.008	
708	1.345i	49.9	4.190	
752	1.354i	49.9	4.340	
709	1.384i	49.8	4.317	
699	1.411i	49.9	F	
700	1.487i	49.9	F	
	AP(N136)[b] 8.4μ			
602	1.074H	50.8	3.713	
590	1.290i	50.8	4.188	
	AP(N126)[c] 25μ			
693	0.901h		2.134	Poor quality charge and trace.
703	1.001h		2.393	
694	1.008h		2.401	
714	1.101h		2.586	
695	1.101h		2.683	
689	1.206i		2.794	
691	1.246i		2.859	
690	1.302i		2.860	
702	1.346i		2.612	Marginal for detonation.
692	1.386i		(2.475)F	

a. Charge length 196.9 mm; all others 228.6 mm
b. See Appendix for additional data
c. d = 50.8 mm, all charges

Table 2

SUBCRITICAL REACTIONS IN 9μ AP(N138)

Mid-Pin Location mm	$\Delta x/\Delta t$ (mm/μsec) ρ_o = 1.59 g/cc	$\Delta x/\Delta t$ (mm/μsec) ρ_o = 1.635 g/cc
25.4	4.47	4.58
50.8	4.39	4.62
76.2	4.43	4.40
101.6	4.37	4.15
127.0	4.17	3.50
152.4	3.64	2.70
177.8	3.42	1.83
203.2	2.43	1.37
228.6	1.93	No reading. Last two inches of tube recovered undamaged except split in two.

Charges in seamless steel tubes 3.65 cm I.D., 4.76 cm O.D., 30.5 cm length.

Booster of 50/50 pentolite (1.56 g/cc), 5.08 cm diam x 5.08 cm long

Pins spaced at 25.4 mm intervals starting 12.7 mm from booster surface

Table 3

RADIUS OF CURVATURE AS A FUNCTION OF DENSITY IN AP

Shot No.	ρ_o (g/cc)	R_c (± % error), mm: Whole Front	R_c (± % error), mm: Middle of Front
	9 μ AP(N138)		
725	0.922H*	70.3(1.57)	97.8(4.47)
734	1.020H*	76.6(1.23)	86.4(2.01)
666	1.075H	75.8(1.52)	81.6(1.69)
667	1.075H	74.5(1.57)	88.8(2.34)
668	1.075H	70.9(1.50)	88.7(2.78)
713	1.191i*	66.3(1.26)	75.1(3.12)
711	1.298i*	67.0(1.35)	76.5(1.82)
748	1.347i*	63.2(1.22)	71.4(1.75)
735	1.376i*	64.9(1.14)	76.3(1.52)
	25 μ AP(N126)		
723	1.001h	51.0(1.17)	56.8(1.72)
724	1.101h	55.2(0.85)	62.3(1.38)
656	1.191i[a]	60.4(1.60)	70.1(1.37)
662	1.258i	53.1(0.96)	63.1(2.41)
674	1.273i[b]	52.0(0.64)	54.9(1.71)
677	1.338i	43.5(0.86)	50.3(1.07)
676	1.339i	44.7(0.82)	49.4(1.68)
685	1.371i[c]	46.8(1.01)	54.7(0.69)

* d = 49.9 mm. For all other charges, d = 50.8 mm
a. 203.2 mm long
b. 457.2 mm long. All others 228.6 mm long
c. This density may be above ρ_c; see Fig. 4.

Table 4

RADIUS OF CURVATURE
vs
CHARGE LENGTH FOR AP

Shot No.	ρ_o (g/cc)*	ℓ (mm)	Apparent D mm/μsec	R_c (± % error), mm From Eq. 2	R_c (± % error), mm From Eq. 1
			9 μ (N138)		
742	1.191	25.4	4.27	74.2(1.12)	74.5(2.2)
743	1.191	25.4	4.27	72.2(1.12)	72.1(2.5)
726	1.193	76.2	4.08	67.8(0.95)	68.5(1.7)
727	1.191	101.2	3.99	69.7(1.25)	68.5(1.4)
728	1.200	127.0	4.05[a]	67.7(1.26)	68.3(1.8)
729	1.191	177.8	3.99	68.8(1.19)	-
713	1.191	228.6	3.99	66.3(1.26)	-
744	1.342	25.4	4.36	72.6(1.29)	73.1(2.0)
745	1.345	76.2	4.36	64.0(1.14)	65.3(2.4)
746	1.358	127.0	4.46	63.6(1.41)	64.4(2.3)
747	1.348	177.8	4.36	63.5(1.10)	-
748	1.347	228.6	4.36	63.2(1.22)	-
			25 μ (N126)		
756	1.296	25.4	3.53	71.9(1.71)	-
757	1.296	76.2	3.62	49.0(0.78)	-
b	1.296	228.6	-	49.3 -	-

---

* All charges prepared in isostatic press; d = 49.9, 50.8 mm for N138 and N126, respectively.

a. Correct to 4.02 for density of 1.191

b. Read from Fig. 6.

Table 5

FRONT CURVATURE FOUND IN SUBDETONATION REACTION OF AP CHARGES

Shot No.	ρ_o(g/cc)	ℓ(mm)	D(mm/μsec)	R_c (± % error) mm	Comment
		9 μ AP(N138)			
753	1.411i	76.2	(4.385)		Obvious curvature
754	1.409i	25.4	4.47*	70.7(1.17)	Trace covers charge diam
755	1.409i	76.2	4.38*	61.0(0.96)	Trace covers charge diam
		26 μ AP(N126)			
683	1.399i	152.4		Not read	Trace covers charge diam
682	1.408i	177.8		Not read	Very faint trace covers only central third of diam
730	1.435i	76.2	2.44*	59.7(0.81)	Trace covers charge diam
731	1.435i	114.3	2.44*	48.9(1.05)	Trace covers only 90% diam; see Fig. 2a

* Shock velocity used in computing R_c

Table 6

RADIUS OF CURVATURE vs CHARGE LENGTH
FOR NQ-ℓ (X547)

Shot No.	ρ_o (g/cc)	ℓ(mm)	ℓ/d	D (mm/μsec)*	R_c (± % error) mm	
					Eq. 2	Eq. 1
774	1.001i	76.1	1.5	5.20	93.7(2.2)	112.0(5.2)
775	1.007i	76.2	1.5	5.23	94.1(2.0)	107.1(5.6)
776	1.001i	127.0	2.5	5.20	91.6(2.4)	103.4(4.7)
777	1.021i	228.6	4.5	5.28	96.1(2.5)	109.0(5.3)
778	1.636i	76.2	1.5	8.01	94.9(1.0)	100.9(3.1)
779	1.653i	76.2	1.5	8.08	90.8(1.0)	93.8(2.8)
780	1.650i	127.0	2.5	8.06	129.6(2.3)	149.7(4.5)
801	1.629i	177.8	3.5	8.00	162.3(3.9)	186.8(13.8)
781	1.645i	228.6	4.5	8.04	166.0(3.3)	205.7(6.0)

* Values of D used in converting t to x data for R_c. All values were computed. At $\rho_o \sim 1$ g/cc, an estimate was made of the diameter effect from difference between ideal value and value measured at d = 25.4 mm. This gave D(1.0 g/cc) ~ 5.2 mm/μsec and 5% less than D_i. The slope of the D_i vs ρ_o curve was then used for further small corrections. At $\rho_o \sim 1.64$ g/cc, D_i was used, (see Ref. 7).

NOLTR 69-235

Table 7

RADIUS OF CURVATURE MEASUREMENTS ON TNT, X517[a]
AT ρ_o = 1.081 g/cc

Shot No.	ℓ (mm)	R_c (mm)[b]		
782	76.2	95.6[c]		
783	76.2	86.6	Av. 92.04	$(\ell/d) = 1.82$
784	127.0	88.1		
785	228.6	97.3		

All charges were 50.8 mm diam and were prepared in the hydraulic press

a. Rotap sieve analysis on 100g sample:

Retained on Screen No.	Wt. (g)
30(590 μ)	0
50(297 μ)	5.20
100(149 μ)	67.20
140(105 μ)	26.50
Pan	0.10
	99.00

Average particle size ca. 200 μ

b. D of 4.8 mm/μsec (about 8% below ideal) used to convert measured time to distance. The larger correction to D_i than that of Table 6 for NQ-ℓ was an estimate for the different charge preparation.

c. Bottom part of this trace was blocked out; cause unknown.

Table 8

EFFECT OF CHARGE LENGTH ON MEASURED D, R_c OF RDX, X659, AT ρ_o = 1.30 g/cc

Shot No.	ρ_o [a] (g/cc)	ℓ (mm)	D (mm/μsec) Apparent	D (mm/μsec) Corrected for Spher. Expansion	D (mm/μsec) Corrected to ρ_o = 1.30 g/cc [b]	R_c (± % error) (mm) By Eq. 2	R_c (± % error) (mm) By Eq. 1
			Pentolite Donor				
771 [c]	1.298	25.4	14.264	6.38	6.39	-	-
760	1.304	76.2	7.470	7.02	7.01	-	-
770	1.300	127.0	7.234	7.08	7.08	-	-
761	1.299	228.6	7.072	7.03	7.03	-	-
764	1.305	25.4	-	-	-	64.3(0.60)	63.0(2.0)
759	1.303	76.2	-	-	-	137.8(1.62)	143.0(7.0)
766	1.302	76.2	-	-	-	123.2(1.18)	134.0(4.0)
767	1.293	127.0	-	-	-	196.5(1.80)	208.0(6.0)
769	1.306	177.8	-	-	-	194.8(4.01)	231.0(8.0)
762	1.302	228.6	-	-	-	270.9(1.58)	296.0(4.4)
			Detonator without Donor				
765	1.300	25.4	-	-	-	39.4(0.65)	34.0(3.0)
768	1.298	127.0	-	-	-	146.4(1.49)	168.0(6.0)
763	1.303	228.6	-	-	-	225.8(1.54)	252.0(6.0)

a) All charges 50.8 mm diam and compacted in the isostatic press
b) Infinite diam value, D_i(1.30 g/cc) = 7.053 mm/μsec. See Ref (16)
c) No booster used

Table 9

NOMINAL REACTION ZONE LENGTHS (z)
COMPUTED FROM EQ. 4

ρ_o (g/cc)	Velocity (mm/μsec) D (d = 50.8) Fig. 4	D_i**	Curvature s(mm) Figs. 6 & 11	Zone z(mm) Eq. 4
		9 μ AP		
0.9	3.23	3.464	75.2	1.45
1.0	3.49	3.722	72.7	1.30
1.1	3.76	3.980	70.3	1.11
1.2	4.01	4.237	67.8	1.04
1.3	4.23	4.495	65.4	1.10
1.35	4.30	4.624	64.1	1.28
		25 μ AP		
1.0	2.38	3.722	50.8	5.23
1.1	2.62	3.980	55.0	5.36
1.2	2.81	4.237	59.3	5.69
1.3	2.83	4.495	48.8	5.15
1.35	2.68	4.624	43.5	5.21
		NQ-ℓ		
1.001	5.2*	5.455	94	1.3
		TNT		
1.081	5.07*	5.318	92	1.2
		RDX		
1.30	7.01*	7.05	130.5	0.21
1.30	7.03*	7.05	270.9	0.22

*Better values needed -- especially for TNT for which (D_i - D) was equated to that found for NQ-ℓ (1 g/cc).
**Respective references are: AP, (12); NQ, (7); TNT and RDX, (16).

APPENDIX

Additional Data on AP's

When NCS* began preparing batches of AP which were obviously finer than the 10 μ average particle size of our initial work[8], one more attempt was made to obtain higher density D vs d data (with $d \leq 7.6$ cm**) which extrapolate to the D_i vs ρ_o curve derived at $\rho_o = 1.0$ g/cc[12]. Table A1 contains the D vs d data for 8.4 μ AP (N136) at 1.074 and 1.30 g/cc. Fig. A1 shows the extrapolation and Table A1 compares the values so obtained with D_i given by the analytical expression of Ref. (12). When the series is terminated at d = 7.6 cm, the extrapolated value is greater than the analytical by 4% at $\rho_o = 1.074$ g/cc and by 12% at $\rho_o = 1.30$ g/cc. These are about the size differences found in the previous work. It should be noted that some of the difference found can be attributed to omitting the correction (now shown inapplicable to AP charges) to the measured D values. If such a correction were used, the difference (at $\rho_o = 1.074$ g/cc) would have been reduced to 2% but would not have been eliminated.

An apparent aging effect (decrease of D) in AP was reported earlier[12]. This has been confirmed by the results on 25 μ AP reported in the text as well as those shown in Table A2 for an 8.8 μ AP. The difference found is small but consistent, a decrease of about 5% in D with age. Differences with age can sometimes be seen in the AP. Thus the N139 of Table A2, although it had been opened only in a dry box or heated in a vacuum oven, showed some caking with age and had to be rolled before making charges 721 and 722. Because we cannot handle this fine AP without causing some agglomeration, henceforth charges will be made from it without any oven treatment of the AP.

---

*Naval Ordnance Station, Indian Head, Maryland.
**Charges small enough to do no damage to our bombproof equipment.

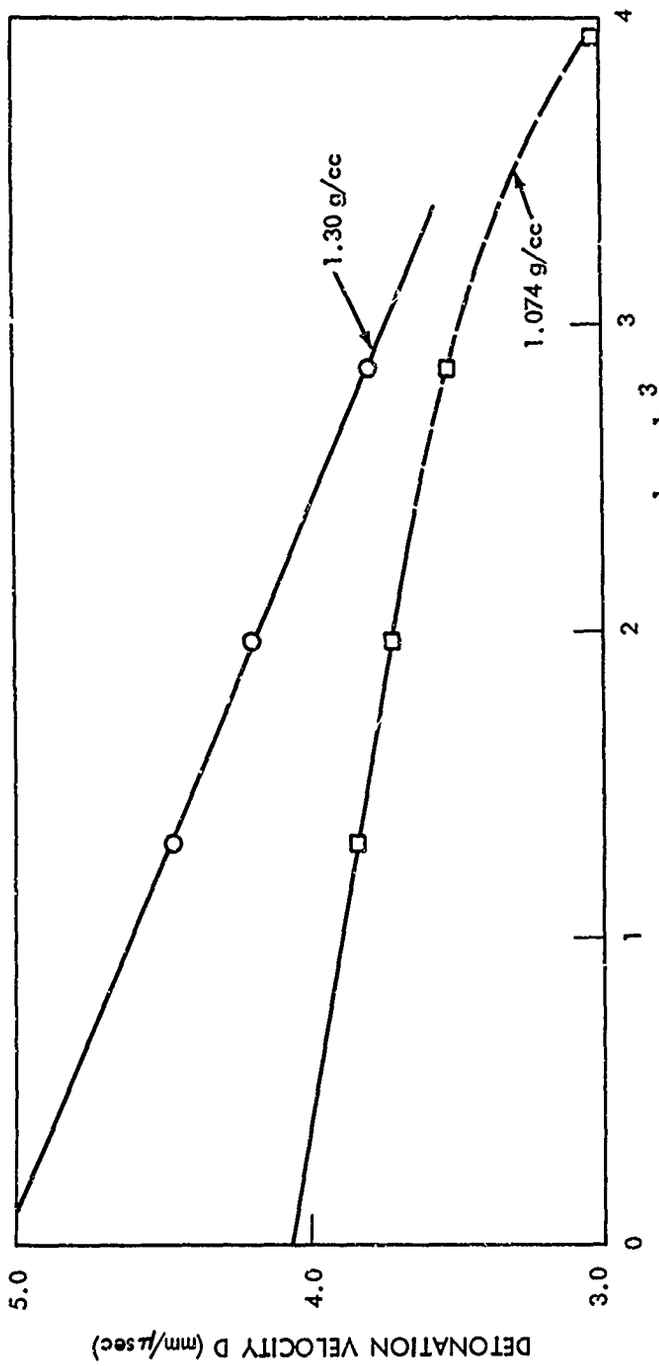

FIG. A1 EXTRAPOLATION OF D VS d^{-1} DATA FOR AP N-136, 8.4 μ

Table A1

D VS d DATA FOR AP(N136), 8.4μ

Shot No.	d (cm)	ρ_o (g/cc)	D(mm/μsec)	D_i mm/μsec Extrap.	D_i mm/μsec Ref (12)
599	2.54	1.072H	3.026		
600	3.495	1.073H	3.525		
602	5.08	1.074H	3.713		
603	7.62	1.073H	3.837		
				4.06	3.91
587	2.54	1.304i	(2.749)F		
588	3.495	1.302i	3.787*		
590	5.08	1.290i	4.188		
591	7.62	1.295i	4.461		
				5.04	4.49

* Poor record.

Table A2

AGING EFFECT ON AP(N139), 8.8 μ

Shot No.	d (mm)	ρ_o (g/cc)	Date	D (mm/μsec)
672	50.6	1.006H	7/10/68	3.466
673	50.6	1.006H	7/10/68	3.508
				Av. 3.49
721	50.8	1.001H	10/25/68	3.315
722	50.8	1.001H	10/25/68	3.292
				Av. 3.30

Charge Length: 228.6 mm

UNCLASSIFIED
Security Classification

DOCUMENT CONTROL DATA - R&D
(Security classification of title, body of abstract and indexing annotation must be entered when the overall report is classified)

1 ORIGINATING ACTIVITY (Corporate author) U. S. Naval Ordnance Laboratory White Oak, Silver Spring, Maryland	2a REPORT SECURITY CLASSIFICATION Unclassified 2b GROUP

3 REPORT TITLE

COMPARISON OF CURVATURE OF DETONATION FRONT IN AP WITH THAT FOUND IN SOME CONVENTIONAL EXPLOSIVES

4 DESCRIPTIVE NOTES (Type of report and inclusive dates)

5. AUTHOR(S) (Last name, first name, initial)

John O. Erkman and Donna Price

6 REPORT DATE	7a. TOTAL NO OF PAGES	7b. NO OF REFS
25 May 1970	59	18

8a CONTRACT OR GRANT NO. ORD-331-002/UF19-332-302 b. PROJECT NO. c d	9a. ORIGINATOR'S REPORT NUMBER(S) NOLTR 69-235 9b. OTHER REPORT NO(S) (Any other numbers that may be assigned this report)

10. AVAILABILITY/LIMITATION NOTICES
This document has been approved for public release and sale, its distribution is unlimited.

11 SUPPLEMENTARY NOTES	12. SPONSORING MILITARY ACTIVITY Naval Ordnance Systems Command

13. ABSTRACT

The original purpose of this work was to obtain data necessary for the design of experiments in which particle velocity (u) could be measured by a new electromagnetic method. It was soon apparent that a knowledge of the curvature of the detonation front was needed for the measurement of detonation velocity as well as for u. Hence, we have studied 50-51 mm diameter charges of AP, NQ, TNT, and RDX to provide the necessary data. The most important result of the work is the finding that the detonation front acquires a constant curvature after a fairly short run in AP charges and also in some low density conventional explosives.

DD FORM 1 JAN 64 1473

UNCLASSIFIED
Security Classification

UNCLASSIFIED
Security Classification

14. KEY WORDS	LINK A		LINK B		LINK C	
	ROLE	WT	ROLE	WT	ROLE	WT
Detonation						
explosive						
ammonium perchlorate						
radius of curvature						
nitroguanidine						
TNT						
RDX						
Tetryl						

INSTRUCTIONS

1. ORIGINATING ACTIVITY: Enter the name and address of the contractor, subcontractor, grantee, Department of Defense activity or other organization *(corporate author)* issuing the report.

2a. REPORT SECURITY CLASSIFICATION: Enter the overall security classification of the report. Indicate whether "Restricted Data" is included. Marking is to be in accordance with appropriate security regulations.

2b. GROUP: Automatic downgrading is specified in DoD Directive 5200.10 and Armed Forces Industrial Manual. Enter the group number. Also, when applicable, show that optional markings have been used for Group 3 and Group 4 as authorized.

3. REPORT TITLE: Enter the complete report title in all capital letters. Titles in all cases should be unclassified. If a meaningful title cannot be selected without classification, show title classification in all capitals in parenthesis immediately following the title.

4. DESCRIPTIVE NOTES: If appropriate, enter the type of report, e.g., interim, progress, summary, annual, or final. Give the inclusive dates when a specific reporting period is covered.

5. AUTHOR(S): Enter the name(s) of author(s) as shown on or in the report. Enter last name, first name, middle initial. If military, show rank and branch of service. The name of the principal author is an absolute minimum requirement.

6. REPORT DATE: Enter the date of the report as day, month, year; or month, year. If more than one date appears on the report, use date of publication.

7a. TOTAL NUMBER OF PAGES: The total page count should follow normal pagination procedures, i.e., enter the number of pages containing information.

7b. NUMBER OF REFERENCES: Enter the total number of references cited in the report.

8a. CONTRACT OR GRANT NUMBER: If appropriate, enter the applicable number of the contract or grant under which the report was written.

8b, 8c, & 8d. PROJECT NUMBER: Enter the appropriate military department identification, such as project number, subproject number, system numbers, task number, etc.

9a. ORIGINATOR'S REPORT NUMBER(S): Enter the official report number by which the document will be identified and controlled by the originating activity. This number must be unique to this report.

9b. OTHER REPORT NUMBER(S): If the report has been assigned any other report numbers *(either by the originator or by the sponsor)*, also enter this number(s).

10. AVAILABILITY/LIMITATION NOTICES: Enter any limitations on further dissemination of the report, other than those imposed by security classification, using standard statements such as:

(1) "Qualified requesters may obtain copies of this report from DDC."

(2) "Foreign announcement and dissemination of this report by DDC is not authorized."

(3) "U. S. Government agencies may obtain copies of this report directly from DDC. Other qualified DDC users shall request through _____."

(4) "U. S. military agencies may obtain copies of this report directly from DDC. Other qualified users shall request through _____."

(5) "All distribution of this report is controlled. Qualified DDC users shall request through _____."

If the report has been furnished to the Office of Technical Services, Department of Commerce, for sale to the public, indicate this fact and enter the price, if known.

11. SUPPLEMENTARY NOTES: Use for additional explanatory notes.

12. SPONSORING MILITARY ACTIVITY: Enter the name of the departmental project office or laboratory sponsoring *(paying for)* the research and development. Include address.

13. ABSTRACT: Enter an abstract giving a brief and factual summary of the document indicative of the report, even though it may also appear elsewhere in the body of the technical report. If additional space is required, a continuation sheet shall be attached.

It is highly desirable that the abstract of classified reports be unclassified. Each paragraph of the abstract shall end with an indication of the military security classification of the information in the paragraph, represented as *(TS), (S), (C), or (U)*.

There is no limitation on the length of the abstract. However, the suggested length is from 150 to 225 words.

14. KEY WORDS: Key words are technically meaningful terms or short phrases that characterize a report and may be used as index entries for cataloging the report. Key words must be selected so that no security classification is required. Identifiers, such as equipment model designation, trade name, military project code name, geographic location, may be used as key words but will be followed by an indication of technical context. The assignment of links, roles, and weights is optional.

UNCLASSIFIED
Security Classification